

605184

RADC-TDR-63-536  
Final Report

COPY 2 OF 3	
HARD COPY	\$ . 4.00
MICROFICHE	\$ . 0.75



104p

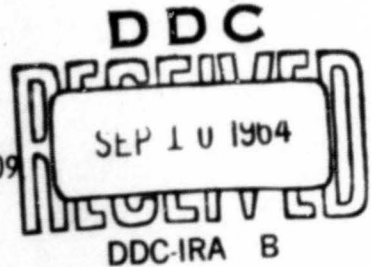
A STUDY OF IMAGE QUALITY EVALUATION

TECHNICAL DOCUMENTARY REPORT NO. RADC-TDR-63-536

August 1964

Information Processing Branch  
 Rome Air Development Center  
 Research and Technology Division  
 Air Force Systems Command  
 Griffiss Air Force Base, New York

System 760H  
 Project No. 6244 , Task No. 624409



(Prepared under Contract No. AF30(602)-3206 by Cornell  
 Aeronautical Laboratory, Inc., Buffalo 21, New York. Authors:  
 Melvin J. Mazurowski, Harry B. Hammill and George H. Snider.)

**BLANK PAGES  
IN THIS  
DOCUMENT  
WERE NOT  
FILMED**

When US Government drawings, specifications, or other data are used for any purpose other than a definitely related government procurement operation, the government thereby incurs no responsibility nor any obligation whatsoever; and the fact that the government may have formulated, furnished, or in any way supplied, the said drawings, specifications, or other data is not to be regarded by implication or otherwise, as in any manner licensing the holder or any other person or corporation, or conveying any rights or permission to manufacture, use, or sell any patented invention that may in any way be related thereto.

Qualified requesters may obtain copies from Defense Documentation Center.

Defense Documentation Center release to Office of Technical Services is authorized.

Do not return this copy. Retain or destroy.

**CLEARINGHOUSE FOR FEDERAL SCIENTIFIC AND TECHNICAL INFORMATION CFSTI  
DOCUMENT MANAGEMENT BRANCH 410.11**

**LIMITATIONS IN REPRODUCTION QUALITY**

ACCESSION # *AD 605184*

- 1. WE REGRET THAT LEGIBILITY OF THIS DOCUMENT IS IN PART UNSATISFACTORY. REPRODUCTION HAS BEEN MADE FROM BEST AVAILABLE COPY.
- 2. A PORTION OF THE ORIGINAL DOCUMENT CONTAINS FINE DETAIL WHICH MAY MAKE READING OF PHOTOCOPY DIFFICULT.
- 3. THE ORIGINAL DOCUMENT CONTAINS COLOR, BUT DISTRIBUTION COPIES ARE AVAILABLE IN BLACK-AND-WHITE REPRODUCTION ONLY.
- 4. THE INITIAL DISTRIBUTION COPIES CONTAIN COLOR WHICH WILL BE SHOWN IN BLACK-AND-WHITE WHEN IT IS NECESSARY TO REPRINT.
- 5. LIMITED SUPPLY ON HAND: WHEN EXHAUSTED, DOCUMENT WILL BE AVAILABLE IN MICROFICHE ONLY.
- 6. LIMITED SUPPLY ON HAND: WHEN EXHAUSTED DOCUMENT WILL NOT BE AVAILABLE.
- 7. DOCUMENT IS AVAILABLE IN MICROFICHE ONLY.
- 8. DOCUMENT AVAILABLE ON LOAN FROM CFSTI ( TT DOCUMENTS ONLY).
- 9.

NBS 9/64

PROCESSOR: *pm*

## **FOREWORD**

The program was monitored by J. A. Stringham of the Rome Air Development Center who was the Air Force Project Engineer. The Cornell Aeronautical Laboratory is grateful for the direction he provided and for the helpful suggestions of other Air Force personnel during the course of the program.

The authors are indebted to the CAL personnel who contributed to the project. In particular, to J. Walker and R. Haas for analyzing and evaluating the test photographs; to R. Kinzly, E. Lindberg, F. Silvestro and J. Sturge for participating in the visual summary measure tests; and to Drs. E. Gerber and P. Roetling for providing helpful suggestions throughout the contract period.

CAL Report Number: VE-1867-G-1

**Suggested Key words: Photo Interpretability; Photographic Analysis**

### **ABSTRACT**

The derivation of an approximate summary measure which would relate measurable photographic parameters to judgments of target interpretability was investigated. An alternative technique for the visual ordering of photographs according to image quality was also studied. Precise and approximate analysis techniques of microdensitometer data for obtaining measures of photographic quality parameters were developed for black and white photography and a brief investigation of the extension of these techniques to color images was conducted. Image quality parameter evaluation techniques are documented and some preliminary attempts to derive summary measure functions are discussed.

### **PUBLICATION REVIEW**

This report has been reviewed and is approved. For further technical information on this project, contact J. Alfred Stringham/EMIIC/4104

Approved:   
ALFRED STRINGHAM  
Project Scientist

Approved:   
FRANK J. TOMAINI  
Chief, Info Processing Branch

FOR THE COMMANDER:   
IRVING J. GABELMAN  
Chief, Advanced Studies Group

## TABLE OF CONTENTS

<u>Section</u>		<u>Page</u>
	ABSTRACT . . . . .	
I	INTRODUCTION . . . . .	1
II	IMAGE QUALITY PARAMETER EVALUATION TECHNIQUES . . . . .	3
	A. Measurement Techniques . . . . .	3
	1. Resolution and Passband . . . . .	4
	2. Determination of Film Granularity . . . . .	9
	B. Approximate Methods . . . . .	16
	1. Edge Traces . . . . .	16
	2. Granularity Traces . . . . .	20
	C. The Determination of Scene Contrast . . . . .	22
III	SUMMARY MEASURES . . . . .	29
	A. Re-Evaluation of Q-CAR Test Photographs . . . . .	29
	B. Correlation of Interpretability Scores and Image Quality Parameters . . . . .	30
	C. Visual Summary Measure . . . . .	32
IV	CONCLUSIONS AND RECOMMENDATIONS . . . . .	39

**TABLE OF CONTENTS (Continued)**

<u>Section</u>		<u>Page</u>
<u>Appendices</u>		
I	PERCENTAGE SCORES FOR RE-EVALUATED PHOTOGRAPHS . . . . .	41
II	DETERMINATION OF LINE SPREAD AND TRANSFER FUNCTIONS FROM AERIAL PHOTOGRAPHS - COMPUTER IMPLEMENTATION . . . . .	45
III	FEASIBILITY OF OBTAINING MEASUREMENTS OF PHOTOGRAPHIC IMAGE QUALITY FROM DENSITY TRACES OF EDGES . . . . .	55
	References . . . . .	75

## LIST OF ILLUSTRATIONS

<u>Figure</u>	<u>Title</u>	<u>Page</u>
1	Smoothed and Unsmoothed Edge Functions . . . . .	10
2	Precision of Resolution Determination . . . . .	11
3	Precision of Passband Determination . . . . .	12
4	Special Relationships of Filtering . . . . .	13
5	Granularity Trace . . . . .	15
6	Construction for Determining Line Spread Function From an Edge Trace . . . . .	18
7	Geometric Construction for the Area Method of Obtaining Passband to Resolution Ratio . . . . .	19
8	Correlation of Passband to Resolution Ratio With a Function of Residual Area . . . . .	20
9	Geometric Construction for the Gradient Method of Obtaining Passband to Resolution Ratio . . . . .	21
10	Correlation of Passband to Resolution Ratio With Rate of Change of Edge Trace Gradient . . . . .	22
11	Illustration of Cylindrical Lens . . . . .	23
12	"Smearing" of Grain Trace by Cylindrical Lens . . . . .	24
13	Contrast as a Function of Number of Scans . . . . .	25
14	Apparent Density Differences for High and Low Passband to Resolution Ratios . . . . .	26
15	Typical Contrast Trace . . . . .	27
16	Correlation of Summary Measure With Percent Score . . . . .	31
17	Optimum Magnification as a Function of Photointerpreter Performance for Different Observers and Criteria . . . . .	34
18	Comparison of Magnifications Obtained by Two Observers Using the Same Criterion . . . . .	35
19	Correlation of Magnifications Obtained by Two Observers Using the Same Criterion . . . . .	37
20	Sampling of Edge Density Trace . . . . .	47

## I. INTRODUCTION

This document is the final report on Project Q-CAR II. The project was conducted at the Cornell Aeronautical Laboratory, Inc. , for the Rome Air Development Center under Air Force Contract No. AF 30(602)-3206. The project involved the determination of an approximate summary measure of photographic image quality, also the concern of an earlier study conducted at CAL for RADC (Air Force Contract No. AF 30(602)-2684).<sup>1</sup>

The objective of the Q-CAR II Project was to accomplish the following tasks:

1. The delineation and documentation of techniques for determining the values of parameters which are descriptive of photographic image quality. These parameters are to be measured from real imagery without recourse to test charts.
2. The analysis of data from the earlier work at CAL<sup>1</sup> as well as from similar work by others to determine an approximate relation between photointerpreter performance and the image quality measures to be used as a quick summary measure.
3. The establishment of a visual technique for obtaining a measure of image quality.
4. The familiarization of RADC personnel with image evaluation techniques including assistance in microdensitometer techniques, computer programming, and the design and use of spatial filtering apparatus.

The first of the above tasks involves the determination of four image quality parameters (resolution, contrast, passband, and granularity) selected on the basis of work done on the earlier contract<sup>1</sup> as being sufficient to describe the various objective aspects of photographic imagery. Procedures have been established for determining these parameters from real imagery without recourse to test charts. Precise and approximate methods of analyses of microdensitometer data have been documented in Section II of this report.

---

<sup>1</sup>Quality Categorization of Aerial Reconnaissance Photography Final Report Contract No. AF 30(602)-2684 CAL Report No. VE-1667-G-1 (Project Q-CAR I)

The second and third tasks described above were continuations of earlier work done at CAL.<sup>1</sup> During this previous program a thousand photographs with a range of quality parameters were generated and used in interpretation tests. A correlation between photointerpreter scores and the image quality parameters was sought but the low scores achieved by the interpreters precluded the derivation of a meaningful summary measure. During the present effort 275 of the modified photographs were re-examined by photoanalysts\* at CAL and relationships sought between various functions of the image quality parameters and the photointerpreter evaluation of the photographs. A possible trend (based upon visual inspection of a scattergram) existed between measures of judged rank of photointerpretability and a summary measure of quality parameters. The modified photographs were also used in tests involving the determination of the optimum viewing magnification for each photograph which was related to judged interpretability to explore the optimum magnification technique as a visual summary measure. It was found that the visual ranking (unaided eye) of the photographs and the judged interpretability of the photographs show greater correlation than does the ranking by optimum magnification.

The familiarization of RADC personnel with image evaluation techniques and with the design and use of spatial filtering apparatus was a continuing process terminating with this final report. Image quality measurement techniques as they existed at the initiation of the present contract, including the use of computer programs, were documented in a memorandum to RADC. The experience gained by RADC in the use of spatial filtering techniques has been documented by Peter Parry<sup>2</sup> (RADC).

Early in the program a study of the extension of the black and white image quality evaluation techniques to color photography was requested by RADC. A brief investigation of the problem was conducted and the results of this study were reported separately to RADC.

---

\* Photoanalysts and photo interpreters are distinguished by a basic training difference. A photo interpreter is trained by the military and has military experience exclusively; whereas a photoanalyst is trained and experienced in civilian applications of photointerpretation, although he may also have had military training and experience.

<sup>2</sup> Parry, Peter D. Image Modification by Spatial Filtering RAW-TM-63-13

## II. IMAGE QUALITY PARAMETER EVALUATION TECHNIQUES

Any combination of parameters selected to represent the quality of a photographic image must represent both the signal and the noise portions of the image. For a photographic system the signal can be represented as the product of the contrast of the objects photographed and the complete system transfer function (i. e. , system contrast modulation as a function of spatial frequency). The noise of a photographic system is represented by the random fluctuations in density due to the granular structure of photographic emulsions. For this and the previous study, four independent parameters were selected.

The signal is represented by the contrast and by two parameters which describe the transfer function. Resolution (R) corresponding to the 25% point of the transfer function describes the extent, and the ratio of equivalent passband (i. e. , the area under the square of the transfer function) to the resolution represents the shape of the transfer function.

While the contrast for any specific target and background can easily be determined from a photograph, this value may obviously not be representative of all target and background combinations in the scene since a whole spectrum of brightness ratios can exist in the real situation. Scene contrast is defined therefore as being representative of the most probable magnitude of density differences for all target background combinations in the scene. That is, a high scene contrast value implies that it is most probable that any specific target and background will have a large density difference while a low scene contrast value implies a high probability that any target background combination in the scene will have a low density difference.

The film granularity ( $\sigma$ ) is defined here as the root mean-square density fluctuation obtained when a uniformly exposed area of the film is scanned with a circular aperture of small area (A).

Techniques for determining the values of resolution, passband, and granularity are described in A below. Methods for determining approximate values of these parameters are presented in B. Various definitions of scene contrast are described in C along with the methods of measuring these values.

### A. MEASUREMENT TECHNIQUES

The first subsection below considers resolution and passband because both are evaluated from the same data, and the second considers granularity which requires separate data.

## 1. Resolution and Passband

Both the resolution and passband are obtained from a microdensitometer scan across an edge within the image format. The following operations are required:

- (a) Selection of an edge for scanning
- (b) Selection of a scanning aperture
- (c) Scanning across the edge to obtain the edge density function
- (d) Data processing to provide resolution and passband.

These four operations are now discussed in detail.

- (a) An edge selected for scanning must be one that results from an edge in the scene whose transition is expected to be sharp compared to the minimum resolvable distance on the ground. Since the resolution of the system is not known, an edge must be selected by inferring that this criterion is met. For present day photographic systems for example, (which achieve ground resolution on the order of one foot at best), the peak of a roof on an ordinary house (which may actually have an edge width of a few inches) provides a satisfactory edge for scanning if no perturbing object such as a chimney is present. If the system can resolve blades of grass, an edge with a much sharper transition (a painted line for example) must be used. The areas on either side of the edge transition should be large compared to the edge width and uniform in brightness so that a uniform exposure in the image will result. The peak of the roof of an ordinary house meets this criteria. A quonset hut, for example, would not provide a satisfactory edge. Although it may appear to have a sharp edge because one side is shadowed, the brightness of the areas on either side of the apparent edge would vary with distance from the edge. Because of the uncertainty of the selection of "good" edges several should be selected and scanned. Only the edges yielding the higher resolution values should be accepted as good sources of the measures.\* To assure that only the linear portion of the H-D curve is utilized, edges whose limiting densities are (by visual inspection) not the limiting densities for the scene should be selected.

---

\* Resolution varies with format position. It has been assumed here that edges have been selected from a limited region of the format such that the resolution is essentially constant.

- (b) There are two considerations for the selection of the scanning aperture. The first is the desirability of using a large area in order to reduce the noise due to grain. The second is the use of a small dimension in the scan direction which prevents further spreading of the edge by convolution with the aperture. This suggests that the aperture be a narrow slit aligned parallel to the edge. The width should be such that a change in width does not visibly affect the edge trace (other than perhaps a change in noise level), but otherwise should be as large as possible to reduce noise due to grain.

There are two factors that will limit the slit length. The first obviously is the length of the edge itself. The ends of the slit should be kept well clear of the ends of the edge in order to assure that the density does not vary along the edge. The second factor is a practical limit depending on the accuracy to which the slit can be aligned with the edge. Where cross-hairs are provided for this purpose, the edge can be visually aligned to within approximately  $0.5^\circ$  to  $1^\circ$ . The edge may be considered to be improperly represented if it is misaligned to the extent that it is parallel to a diagonal of the scanning slit. The alignment accuracy of  $0.5^\circ$  to  $1^\circ$  therefore suggests an 80:1 ( $\cot 0.75^\circ$ ) length to width ratio. If the ratio of length to width of the slit exceeds 80:1, a substantial increase in the effective width in the scan direction will result from a small error in the alignment angle.

The procedure for determining the proper slit is a matter of trial and error. A slit is selected initially whose length is less than the length of the edge (less than  $2/3$  the edge length). The width is changed for each scan until the maximum width that does not visibly affect the shape of the density trace is found. During these scans the length to width ratio should not exceed 80:1 in order that alignment problems do not occur.

Once the proper slit width has been determined, the maximum length should be found (again by trial and error) such that the density trace again remains unaffected, other than a change in the noise fluctuations in the trace.

It should be pointed out that the slit dimensions discussed above are bounds on the dimensions that will provide low noise with a minimum of distortion to the desired edge function. In practice, the final selection of slit dimensions will be limited by those slits available for scanning. In any event the bounds should not be exceeded.

- (c) After the proper slit has been selected and aligned, the final scan from which the resolution and passband will be determined can be made. The scan should extend far enough on either side of the edge to guarantee that the portion desired for processing will be included. If neighboring objects on either side of the edge are included in the scan, it will be easier to identify the trace with the image itself, thus aiding in the decision of which portion is to be used for processing.
  
- (d) The measures of resolution and passband are computed from the density trace with the aid of a computer. The processing is accomplished as follows:
  - (1) Sampling of the density trace for computer input
  - (2) Smoothing of input data to reduce fluctuations due to grain
  - (3) Calculation of the line spread function
  - (4) Calculation of the passband
  - (5) Calculation of the transfer function from which the resolution is determined.

With the exception of Steps (1) and (2), the processing is routine and is discussed in detail in Appendix II. The remainder of this section will be concerned with sampling and data smoothing.

The primary problem in providing a set of data to the computer for analysis is the decision of where on the density trace to start and end the sampled section. If there are no other objects in the vicinity of the scanned edge, there will be no interference problem and the ends should be selected where the density trace (excluding noise) appears constant to the eye. If interfering objects are present, it is necessary to terminate the sampling closer to the edge. This premature termination will give rise to errors in the computed values of resolution and passband. In both a recently completed internal research program<sup>3</sup>, and the present program (Q-CAR II), edges were found whose density traces possess long "tails" of finite slope (due to a line spread function with long tails). Such traces (indicative of a low ratio of passband to resolution) often give rise to errors due to termination.

---

<sup>3</sup> Feasibility of Obtaining Measurements of Photographic Image Quality from Density Traces of Edges, Final Report, Internal Research Study CAL-132

Once the terminating points have been selected, the density trace within these points is sampled at approximately 50\* equally spaced points. The use of less than 50 points may cause the shape of the edge to be poorly represented. There is certainly no disadvantage to using more than 50 points except for the time spent in the sampling and the preparation of the computer input data.

As discussed previously, the fluctuation in the density trace due to film grain is reduced by making the scanning aperture as large as possible. The aperture thus provides some smoothing prior to sampling which reduces the number of samples required to represent the function but lacks the flexibility of numerical smoothing techniques. The scanning aperture often does not reduce the fluctuation to a level small enough that Steps (3), (4), and (5) can be carried out to provide satisfactory values of resolution and passband. Additional smoothing is required which can be accomplished in two ways:

- (a) Hand Smoothing - Prior to sampling, a smooth curve is drawn through the noisy density trace, and the smoothed curve sampled for computer input. An analysis of how well this method extracts the signal from the signal plus noise is difficult since the smoothing is subjective. It has the advantage that it provides a "quick look" at the density trace, but the disadvantage that it is often biased.
- (b) Numerical Smoothing - The use of a computer in the natural course of calculating the measures of resolution and passband allows, with little effort, complex smoothing of the noisy density trace by numerical techniques. Two numerical methods have been utilized to provide smoothing; a least squares fit of a polynomial, and linear filtering.

The first smoothing routine is the least squares fitting of a polynomial to the sampled density trace. The degree of the polynomial was varied and a 7th degree was selected as a compromise between poor fitting of lower degree polynomials and the poor "noise filtering" of polynomials of higher order. With a fifth degree polynomial, for example, it was noted that in both the high gradient portion and at the ends of the density trace, the slope of the fitted polynomial deviated considerably from that of the trace. For these reasons, the derivative of the density trace and the trace itself, were fitted with a 7th

---

\* The choice of 50 points was made on the assumptions that edges usually cannot be traced far beyond the region of maximum transition. Clearly in the case of test edges where large constant regions are available many more than 50 points would be needed for adequate representation.

degree polynomial with special emphasis on the derivatives of the end points. This leads to a least square error\* which can be written as the weighted sum of three square errors. The total error is then minimized with respect to the polynomial coefficients. The use of a polynomial fitted in this manner yielded a definite improvement over the polynomial fitted to the density alone.

A second technique for data smoothing is linear numerical filtering.<sup>4</sup> The procedure is to compute a smoothed value for each density value in the sample from a linear combination of the other sample points. This is equivalent to a convolution of the noisy density trace with a function which is characteristic of a low pass filter. In this manner the high frequency fluctuations are greatly reduced, while the edge trace (predominantly low frequencies) undergoes minor distortion. There are two considerations in designing this filter; the shape of the function, and the cut-off frequency. Preliminary trials have indicated that the shape is of minor importance but the cut-off frequency should be selected with care. Again, as with the microdensitometer scanning aperture, too high a cut-off frequency will not filter out the noise and too low a frequency will excessively distort the signal.

The linear filter selected yields the following smoothed density values;

$$D_s(\chi_k) = \frac{1}{\sum_{j=-n}^n (n - |j| + 1)} \cdot \sum_{j=-n}^n D(\chi_{k-j}) (n - |j| + 1)$$

where:

$D(\chi_k)$  = raw density value from trace at kth sample point

$D_s(\chi_k)$  = density value after smoothing at kth sample point

$n$  = scale factor

---

\* Appendix II

<sup>4</sup> An Exploration of Numerical Filtering Techniques, CAL Internal Research Report No. XA-869-P-1

The cut-off frequency is controlled by the parameter  $n$ . As the parameter  $n$  is increased, the cut-off frequency will become lower.

As an example of the smoothing, Figure 1 shows a truncated density curve (corresponding to a gaussian transfer function) including random noise. The smoothed density curves for both the fitted polynomial and the linear filter ( $r = 4$ ) are included. The effectiveness of the 7th degree polynomial fitting and linear numerical filtering just described were compared by using each technique to analyze a series of edge traces derived for systems with known transfer functions. Two density curves were used; one corresponding to a gaussian transfer function and the other to an exponential transfer function. The density curves were truncated to provide a reasonable region for sampling and each was used many times with independent random noise samples added. The values of  $R$  and  $N_e$  obtained by using the polynomial and the linear filter were compared to the correct values as determined under the conditions of no noise and no smoothing. This comparison to the true values\* is shown in Figures 2 and 3 where the results for edges with high values of noise and low values of noise are separated to simplify the figures. For the cases considered, the overlapping of the bands in these figures for the polynomial fitting and the linear filtering techniques indicate no preference for one technique over the other.

## 2. The Determination of Film Granularity

Granularity<sup>1</sup> is a function of the emulsion used, the developing process, the average density level and the spatial frequencies over which it is measured. The first two factors are not involved in the measurement process and therefore need not be considered. The third factor can be taken into account most readily by making the granularity measurement at approximately the average image density<sup>1</sup>. While the grain noise of photographs other than originals can be a function of spatial frequency, the grain spectrum of original photographs is very nearly constant. In controlled experiments, where film is exposed using a uniform light source, only the grain spectrum is present in the developed image. Continuing analysis of film granularity has shown that real imagery frequently contains a small amount of signal power even in an apparently uniform area. The effect of the presence of this signal is to increase the value of

---

\* The "true values" are those for the theoretical truncated function, and therefore are not values expected if the theoretical curve were continued to infinity (See Reference 3)

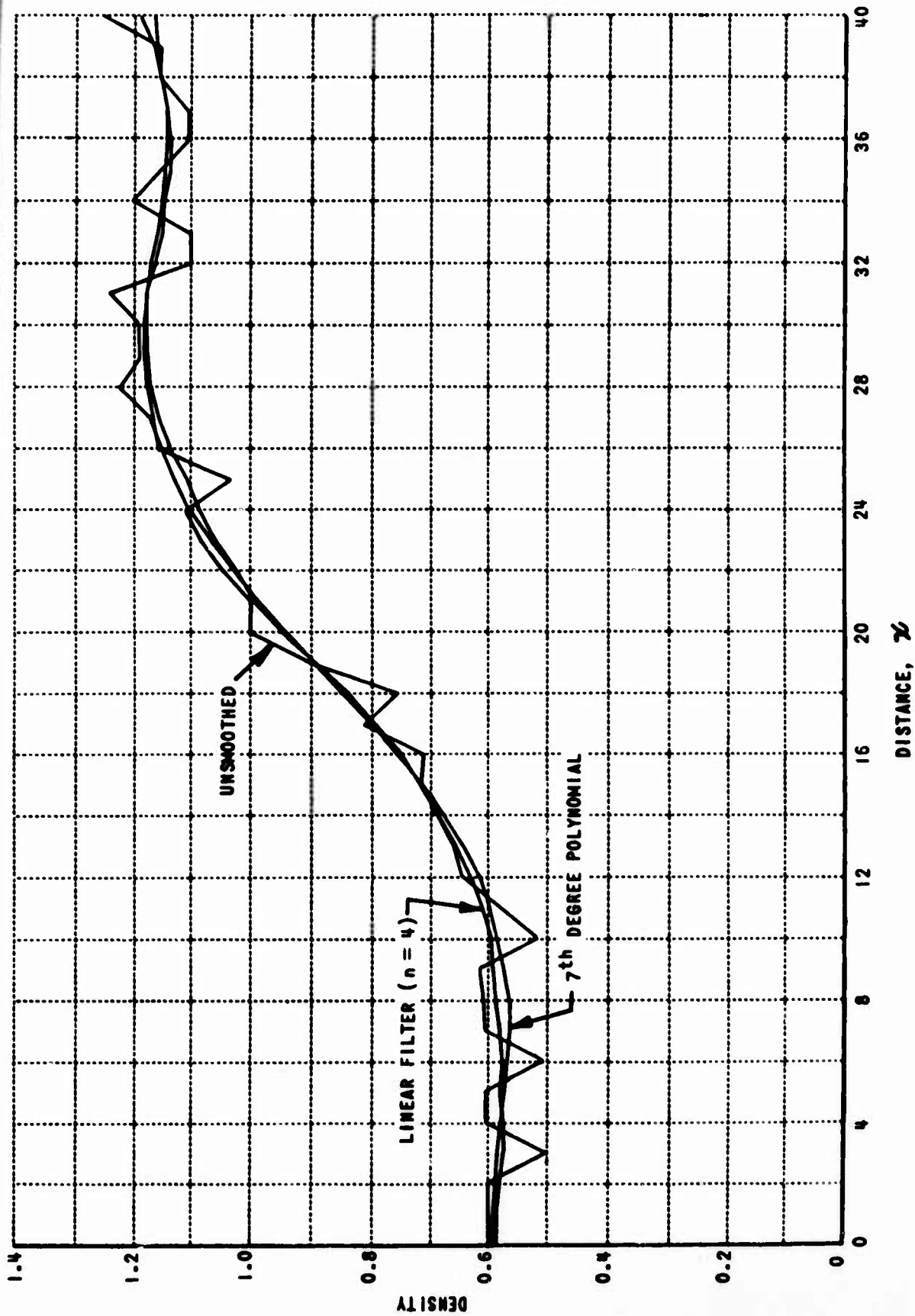


Figure 1. Smoothed and Unsmoothed Edge Functions

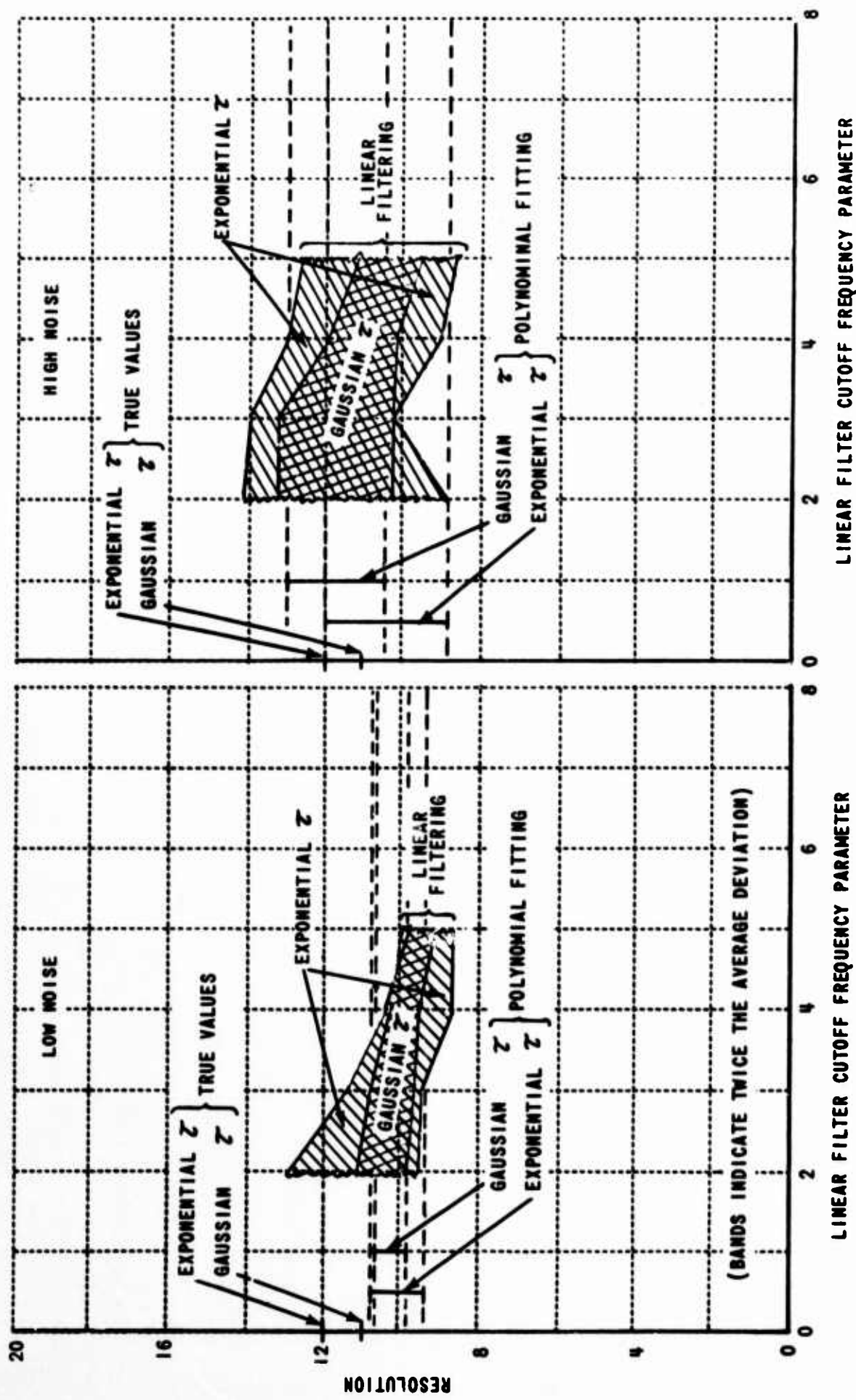


Figure 2. Precision of Resolution Determination

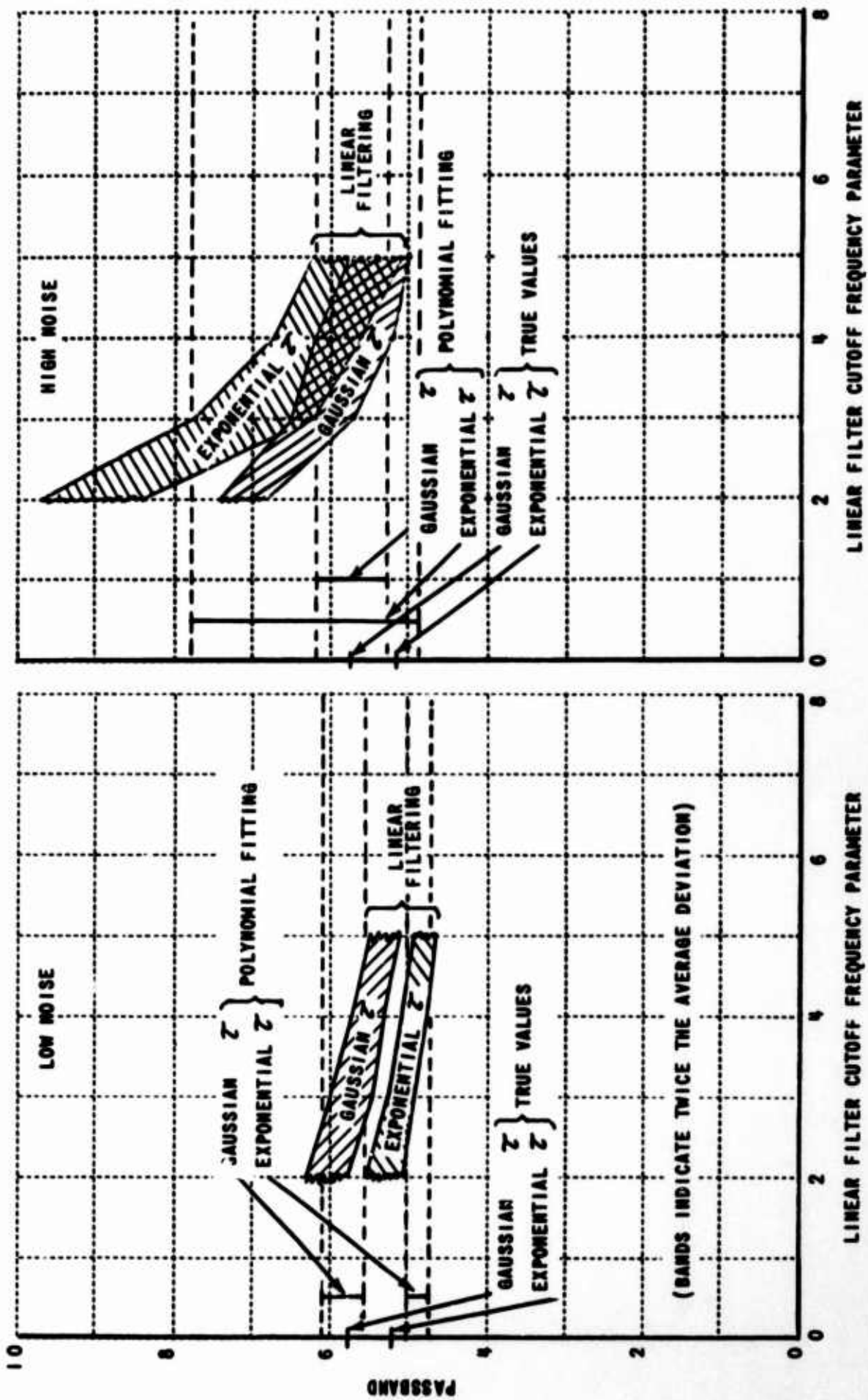


Figure 3. Precision of Passband Determination

$\sigma$  obtained, especially for low grain films. This is illustrated in Figure 4. A small, low frequency signal spectrum (dotted curve) is shown superimposed on a flat grain spectrum (solid line). Since  $\sigma$  is in a sense a measure of the area under the composite curve (after multiplication by the scanning aperture frequency response), the small signal causes an increase in the measured value of  $\sigma$  that is dependent upon the ratio of noise to signal. The effect of this residual signal can be removed, however, by using numerical filtering techniques<sup>4</sup> to weight the data so that only the contributions from spatial frequencies above  $\nu_c$  are included. The response curve of this "filter" (dotted line) is also shown in Figure 4. It is clear from Figure 4 that the numerical filtering technique removes a part of the grain spectrum as well as the residual signal spectrum. The value of  $\sigma_F$  obtained after filtering is thus lower than the true value but is not affected by the presence of varying amounts of signal. The filtered value of  $\sigma_F$  can be corrected to the true value by multiplying it by the theoretical ratio,  $\rho_F$ , of an arbitrary rms density fluctuation expected for an unfiltered flat grain spectrum to that rms value expected after filtering with a specific filter.

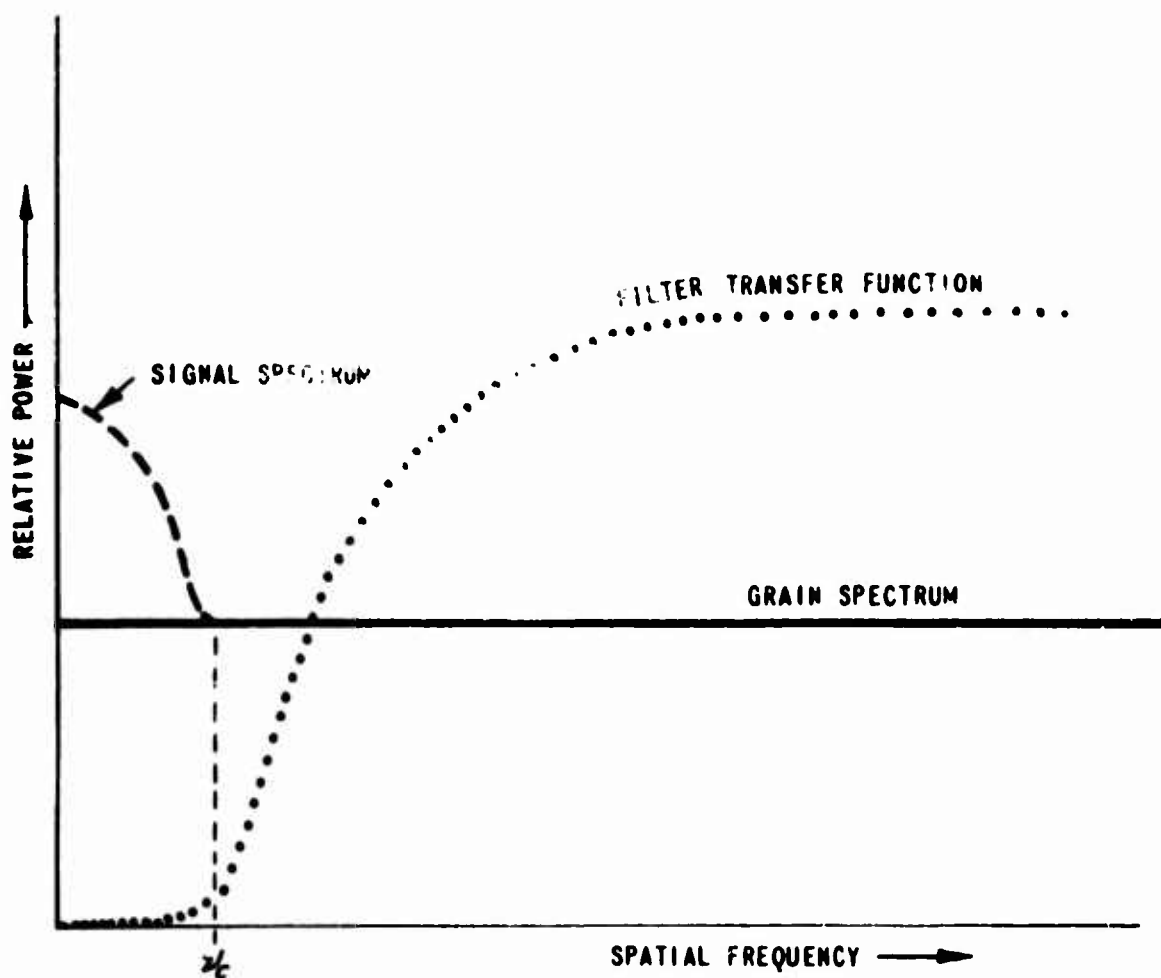


Figure 4. Spectral Relationships of Filtering

**Granularity can thus be determined in the following manner:**

- (a) A uniformly exposed area whose density approximates the scene average is selected by visual inspection.**
- (b) The selected area is scanned with a microdensitometer equipped with a digital output device and using a small circular aperture (a  $10 \mu$  diameter circle was used at CAL for convenience. Kodak uses a  $24 \mu$  diameter aperture\*).**
- (c) During the scan which results in a trace such as shown in Figure 5, the density is sampled at a rate of from 1 to 2 samples per effective aperture diameter, converted to digital form and punched on paper tape, cards, or fed directly into a computer. Approximately 1000 points should be taken in this manner. This implies that a uniform area in the image must have a dimension of at least 5 to 10 millimeters. Where this is not possible, a series of scans can be made across the uniform area along parallel lines at least one aperture diameter apart.**
- (d) The average density and the root mean-square density fluctuation ( $\sigma$ ) of all the data points are then determined.**
- (e) All of the data points outside of  $2\sigma$  are then discarded to avoid the inclusion of transient and unusually large fluctuations in density due to scratches and dust spots. A new average density is computed for the remaining points.**

---

\* The root mean-square density fluctuation,  $\sigma$ , is related to the area of the scanning aperture by  $\sigma = G \cdot A^{-1/2}$ , where G is a constant for any given film called the Selwyn granularity constant. The value of  $\sigma$  obtained with a given aperture can thus be related to that for a different aperture by  $\sigma_1 D_1 = \sigma_2 D_2$  where D is the diameter of the aperture.

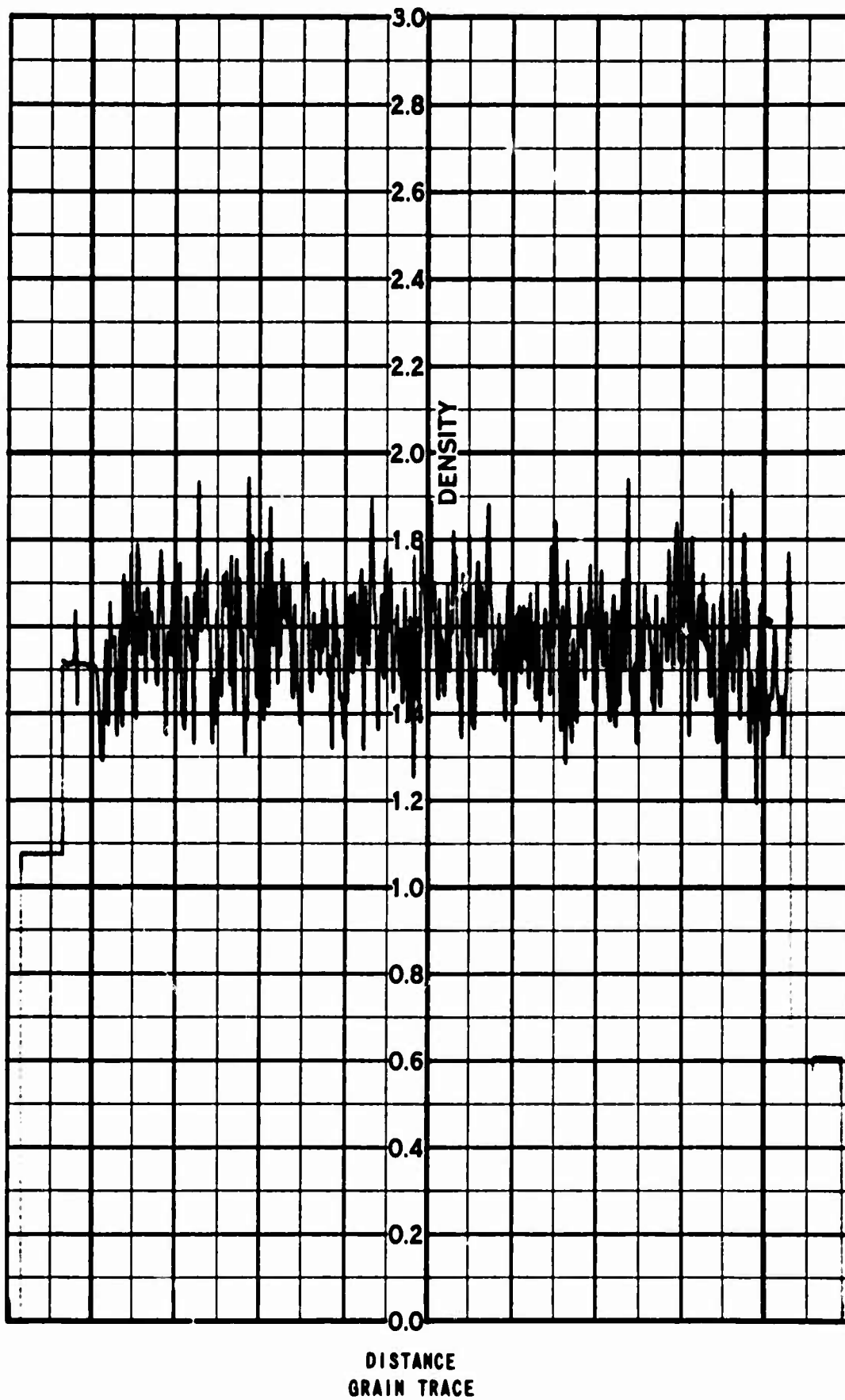


Figure 5. Granularity Trace

- (f) To eliminate low frequency data which may be present due to a small residual image "signal", the remaining points are weighted using numerical linear filtering techniques and the root mean-square fluctuation of the weighted points ( $\sigma_F$ ) is computed. The actual value of  $\sigma$  can then be computed by multiplying by  $\rho_F^*$ .

## B. APPROXIMATE METHODS

The previous sections considered image quality parameter evaluation techniques which utilize a computer in the analysis of microdensitometer scans. This section concerns techniques wherein simple geometrical analyses of the same density traces are used to obtain a quick, though perhaps less accurate, evaluation of the same image quality parameters.

### 1. Edge Traces

The relationship between the slope  $D'(\chi)$  of a density trace from the scan of an edge and the line spread function of the system,  $L(\chi)$ , presented in Reference 1 and in Appendix II of this report can be approximated<sup>3</sup> as:

$$L(\chi) = \frac{D'(\chi)}{\Delta D} \quad (1)$$

\*At CAL granularity was measured using a  $10 \mu$  diameter aperture. The density was sampled every  $5.56 \mu$  by scanning at 2 mm/min and sampling 360 times per minute. After eliminating the data outside of the  $2\sigma$  point, the remaining points were weighted in the following manner. Each weighted point  $D'_k$  was computed from the data point  $D_k$  using  $D'_k = \sum_{n=-4}^4 W_n D_{k+n}$

where:

$$W_{-4} = W_4 = -0.00391$$

$$W_{-3} = W_3 = -0.03125$$

$$W_{-2} = W_2 = -0.10938$$

$$W_{-1} = W_1 = -0.21875$$

$$W_0 = +0.72657$$

For this filter  $\nu_c = 30$  lines/mm and  $\rho_F = 1.23$ .

where  $\Delta D$  is the difference between the upper and lower density limits of the edge trace. In Reference (1) a correlation between the maximum value of the line spread function and the resolution was presented which resulted in the empirical relationship

$$L(\chi)_{\max} = 1.45R \quad (2)$$

Equations (1) and (2) can be used to obtain an approximate value of both the resolution and the passband to resolution ratio of a photographic system directly from the density trace. Figure 6 shows a typical density trace with a line drawn tangent to it at one point. From Figure 6,

$$D'(\chi) = \frac{\Delta D}{\Delta \chi}$$

and therefore from Equation (1)

$$L(\chi) = \frac{1}{\Delta \chi} \quad (3)$$

Combining Equations (1), (2) and (3) yields

$$R = \frac{1}{1.45 (\Delta \chi)_{\min}} \quad (4)$$

The resolution of a system can thus be determined by drawing a tangent through the point of maximum slope of the edge trace, determining the distance  $\Delta \chi_{\min}$  in millimeters from the scale of the microdensitometer chart paper and computing the resolution using Equation (4).

The passband of a system is defined to be the area under the square of the line spread function<sup>1</sup>. Thus, for a given resolution the passband and hence the passband to resolution ratio decrease as the line spread function becomes wider at low values of  $L(\chi)$  and correspondingly narrower at high values of  $L(\chi)$  since the area under  $L(\chi)$  is defined to be unity (i. e. , as the energy becomes spread over a greater distance). From Equation (1) it can be seen that this "spreading" of  $L(\chi)$  implies that as passband decreases, the density trace of an edge also tends to "spread" as indicated by the dashed line in Figure 6. This effect suggests two possible means of approximating the passband to resolution ratio from simple geometric considerations.

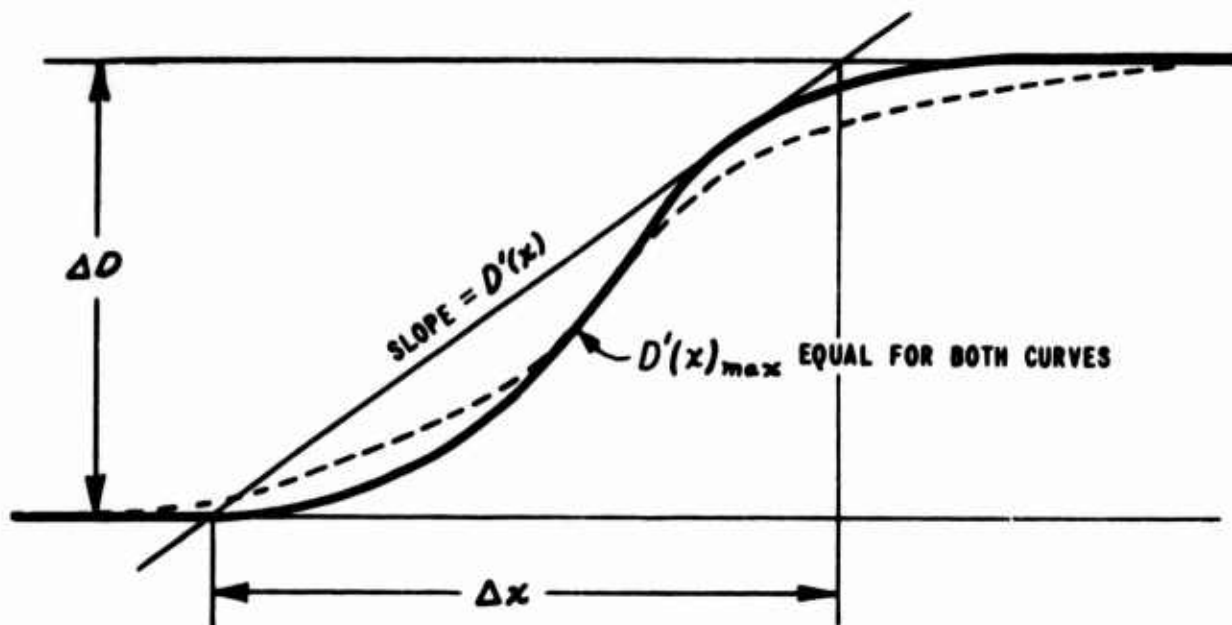


Figure 6. Construction for Determining Line Spread Function from an Edge Trace

Consider the area bounded by the edge trace, the lines of minimum and maximum density, and a tangent drawn through the point of maximum slope of the edge trace. This area,  $a$ , is illustrated in Figure 7 and it should increase with a decrease in passband, a decrease in resolution and an increase in  $\Delta D$ . It is plausible that one method of estimating the passband to resolution ratio of a system could be based on a relationship between  $N_e/R$  and  $a$ .

A series of edge traces for which the passband to resolution ratio was known were used to evaluate the feasibility of using this method to predict  $N_e/R$ . The areas were approximated as triangles, their area (in density units-millimeters) determined, and a quantity  $a'$  computed (normalized to the  $\Delta D$  and  $R$  values) as:

$$a' = \frac{a (\text{Density} - \text{millimeters}) \cdot R (\text{millimeters}^{-1})}{\Delta D (\text{density})} \quad (5)$$

The values of  $a'$  obtained from several real and several theoretical edge traces were plotted as a function of their passband to resolution ratio (Figure 8).

Although the points are scattered, a definite trend exists. That is, larger values of  $a'$  are obtained for low  $N_e/R$  edges than for high  $N_e/R$  edges. The technique described above can thus be used to obtain a value for  $a'$ , and a value of passband to resolution ratio can be estimated from the line in Figure 8.

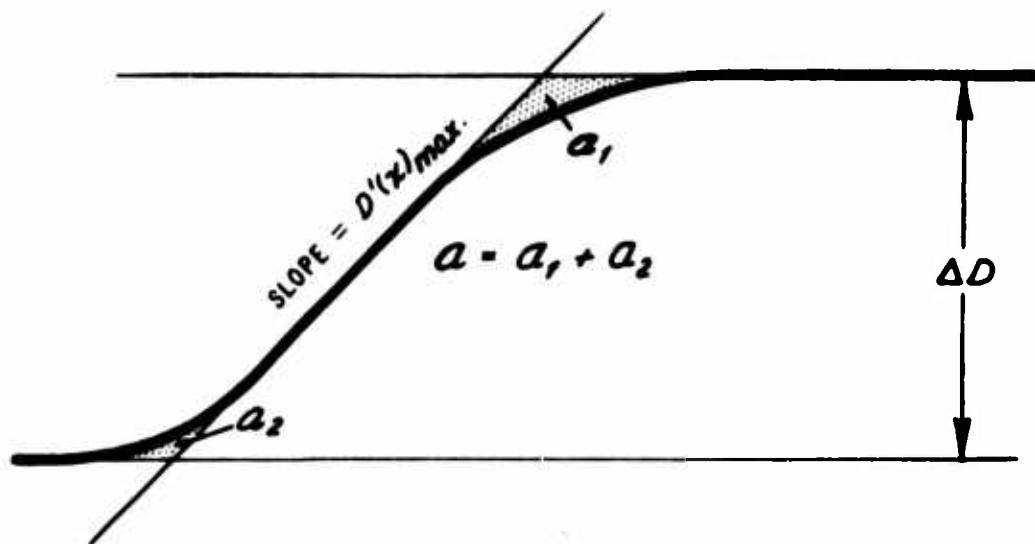


Figure 7. Geometric Construction for the Area Method of Obtaining Passband to Resolution Ratio

The second suggested method relates a measure of the rate of change of the width of the line spread function at low values of  $L(x)$  to the passband to resolution ratio. Several measures of the width of the line spread function at various fractions of  $L(x)_{\max}$  were tested and the ratio of the width of  $L(x)$  at  $1/8 L(x)_{\max}$  to the width of  $L(x)_{\max}$  was found to provide the best correlation with  $Ne/R$ . As implied by Equations (1) and (3) this ratio can be obtained directly from the density trace by locating the points along the trace at which the slope is  $1/8$  and  $1/4$  of the maximum slope, as illustrated in Figure 9, and measuring distances  $\Delta x_{1/4}$  and  $\Delta x_{1/8}$ . A plot of the ratios of  $\Delta x_{1/8}$  to  $\Delta x_{1/4}$  determined for the same traces mentioned above, is shown as a function of  $Ne/R$  in Figure 10. Again, despite the scatter, it can be inferred from this figure that a definite trend exists and that therefore  $Ne/R$  can be estimated using the technique described above to compute the ratio  $\Delta x_{1/8}$  to  $\Delta x_{1/4}$  and by then referring to the line in Figure 10.

Since a considerable amount of spread exists in the determination of  $Ne/R$  by either proposed methods, the estimate of  $Ne/R$  should probably be obtained by using both methods and averaging the results.

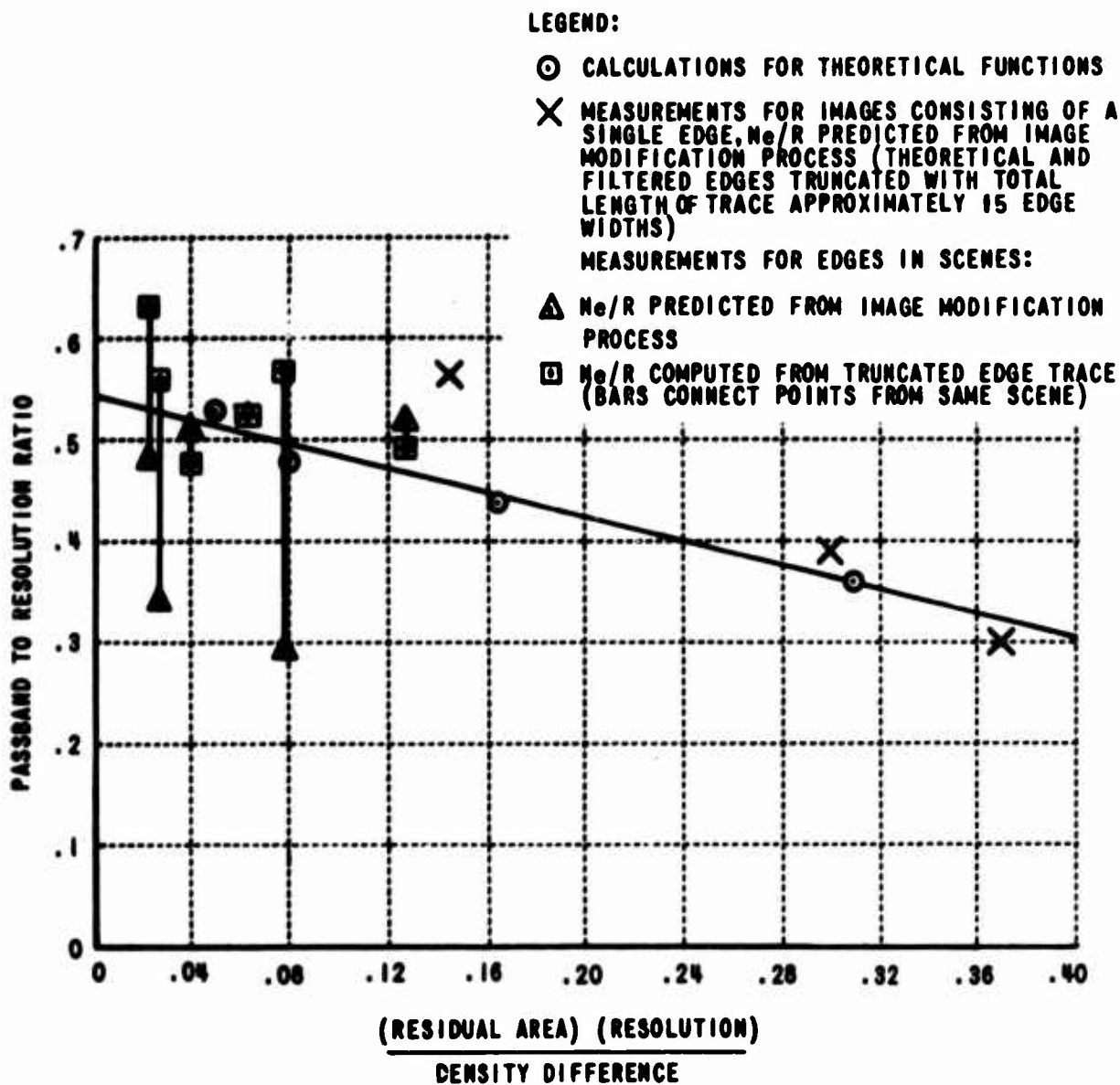


Figure 8. Correlation of Passband to Resolution Ratio with a Function of Residual Area

## 2. Granularity Traces

A method for estimating the rms density fluctuations obtained when a scan across a uniformly dense area of a photograph is made as described in Section II A 2 has been devised and is explained here.

While direct examination of a trace such as that shown in Figure 5 does convey the impression of these density fluctuations, the observer's impression of the fluctuations is strongly affected by the peak to peak density differences. The directional image smearing properties of a cylindrical lens can be used to determine the rms density fluctuations in the following manner.

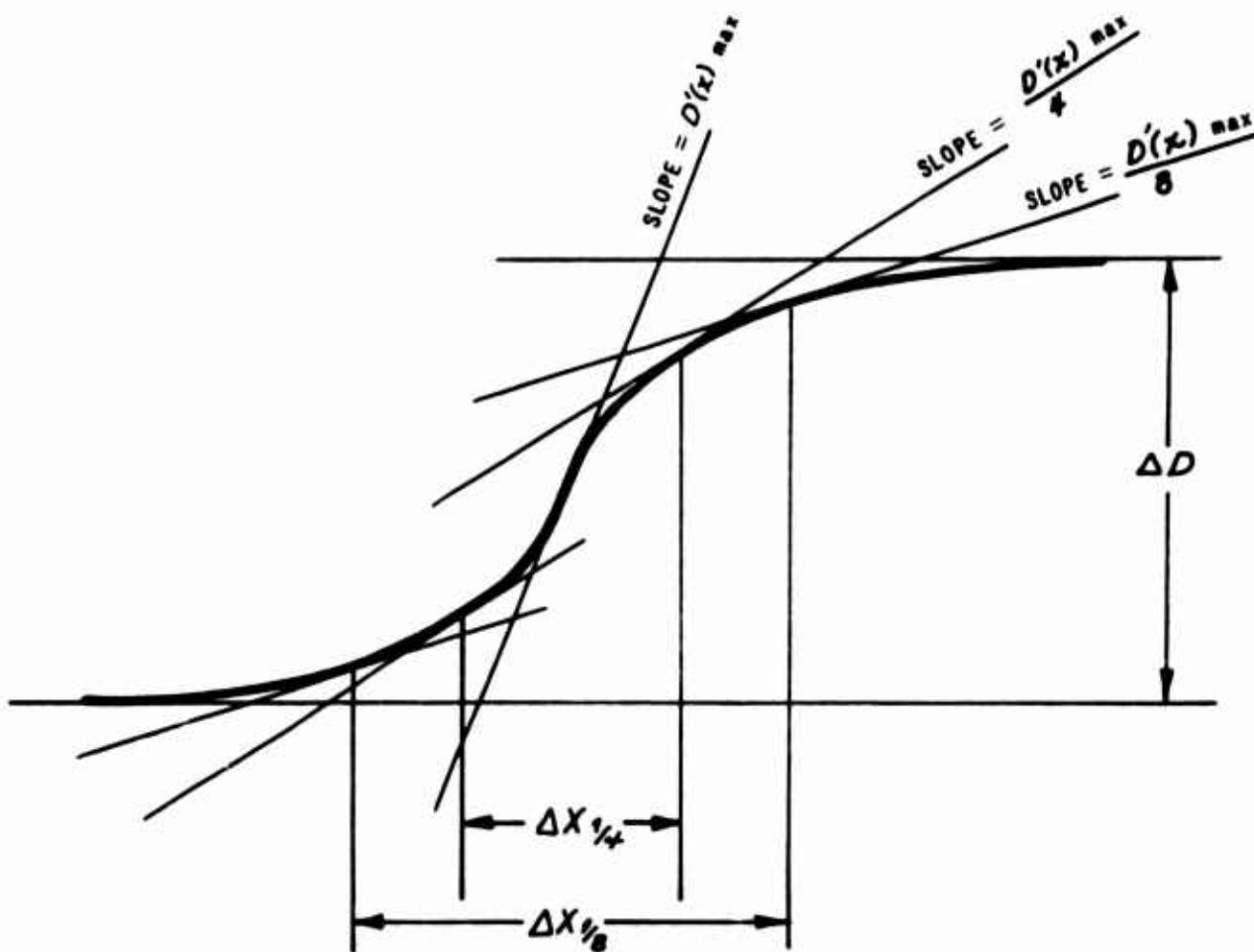


Figure 9. Geometric Construction for the Gradient Method of Obtaining Passband to Resolution Ratio

The trace is viewed through a cylindrical lens which has its "smearing axis" as shown in Figure 11 perpendicular to the density scale.

The lens should be held at a distance from the trace of approximately 10 times the focal length or more and the eye should be placed at a distance from the lens about equal to the focal length. The trace will appear "smeared" (in the direction of the scan) into a band as shown in Figure 12. The width (in density units) of the dense area of this band is determined from the density scale of the chart paper. \* A series of tests conducted using a variety of grain traces has shown that the width of this band is approximately equal to  $2\sigma$  where  $\sigma$  is the rms density fluctuation as defined in Section II A 2 of this report.

\* Lines of constant density will be parallel to the smearing axis of the lens and thus will not appear to be smeared as is illustrated in Figure 12.

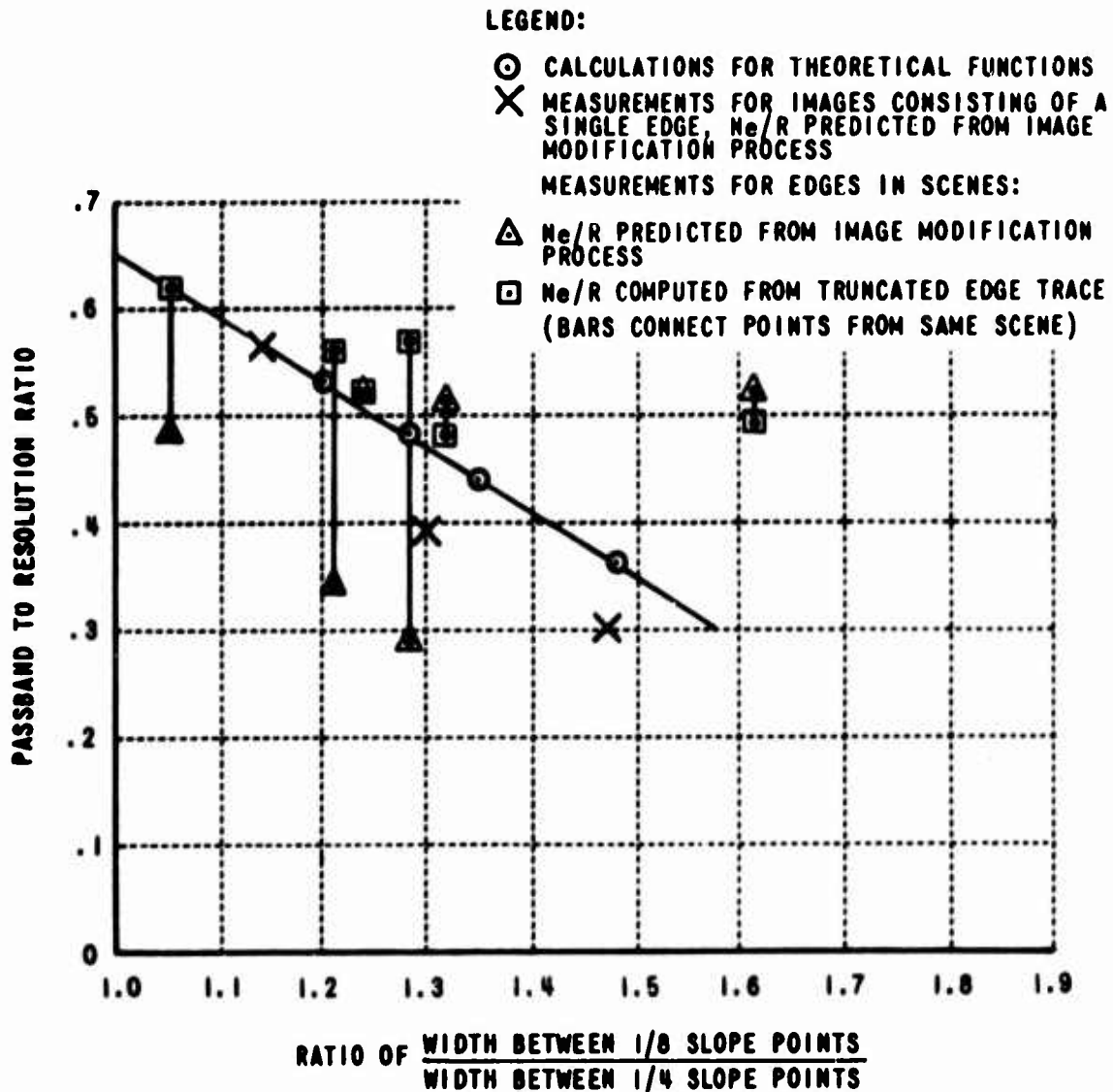


Figure 10. Correlation of Passband to Resolution Ratio with Rate of Change of Edge Trace Gradient

### C. THE DETERMINATION OF SCENE CONTRAST

As discussed earlier the value of contrast necessary for use as a quality parameter for aerial photographs must be representative of the entire scene. In the earlier study<sup>1</sup>, scene contrast was the average of the six largest monotonic density differences occurring in a single microdensitometer trace across the image format through a representative portion of the photograph. This definition yields a value of scene contrast which is dependent not only upon the contrast rendition of the photographic system (atmosphere included) but also upon the density fluctuations due to specific objects in the image. Hence, the value of scene contrast obtained in this manner is useful for comparing

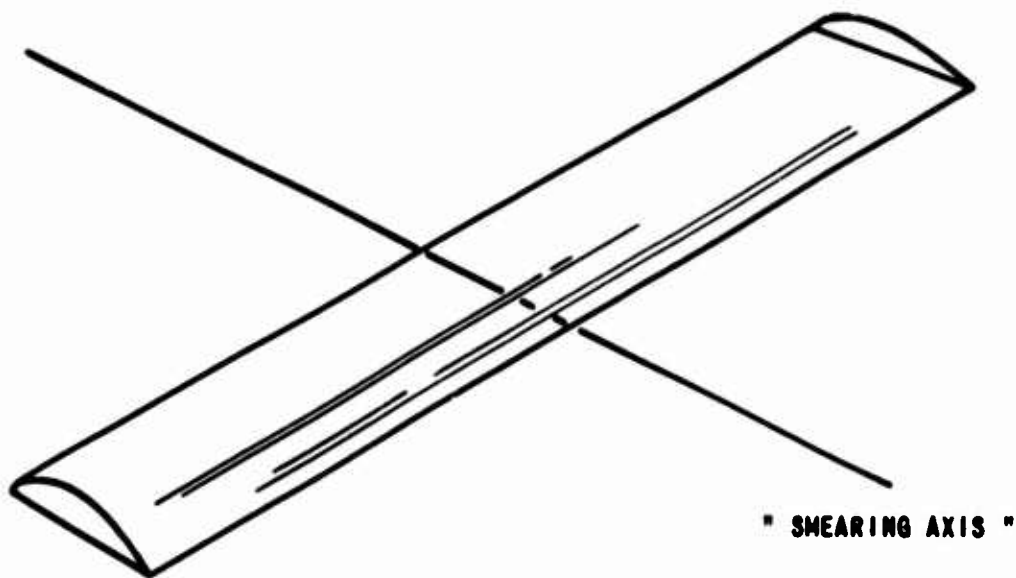


Figure 11. Illustration of Cylindrical Lens

scenes with the same general class of targets. That is, tactical areas might not be expected to yield the same results as a highly detailed area such as an airport because the inherent contrast of nearby objects in each of these scenes can be quite different.

A brief analysis of the repeatability of this type of measurement was conducted during the previous image evaluation study<sup>1</sup>. A  $\pm 15\%$  probable error was found. During the present program a more thorough analysis disclosed that differences as large as 50% can occur quite frequently and that the probable error for a single scan sample is  $\pm 30\%$ . This analysis has shown that by using the data from at least 5 scans across the entire photograph a value of scene contrast repeatable to  $\pm 15\%$  can be obtained. Since many more than 5 scans are required to significantly reduce this error, scene contrast should be measured in future programs by using 5 scans across the photograph. The effect on the repeatability of the contrast measure of including the density differences from a larger number of scans is illustrated in Figure 13 where the scene contrast value (with the standard deviation in the value) is shown as a function of the number of scans used to obtain the six highest peaks.

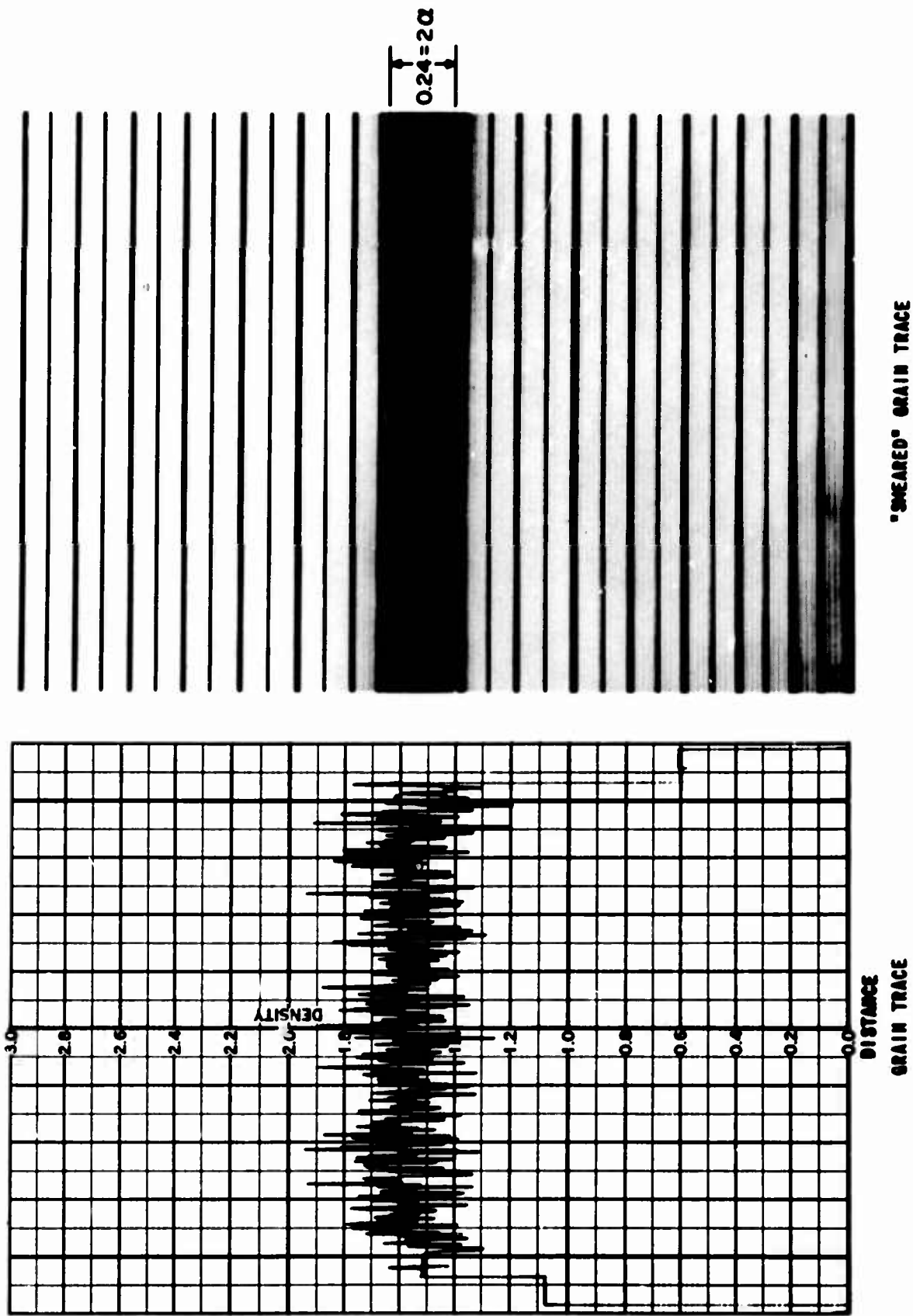


Figure 12. "Smearing" of Grain Trace by Cylindrical Lens

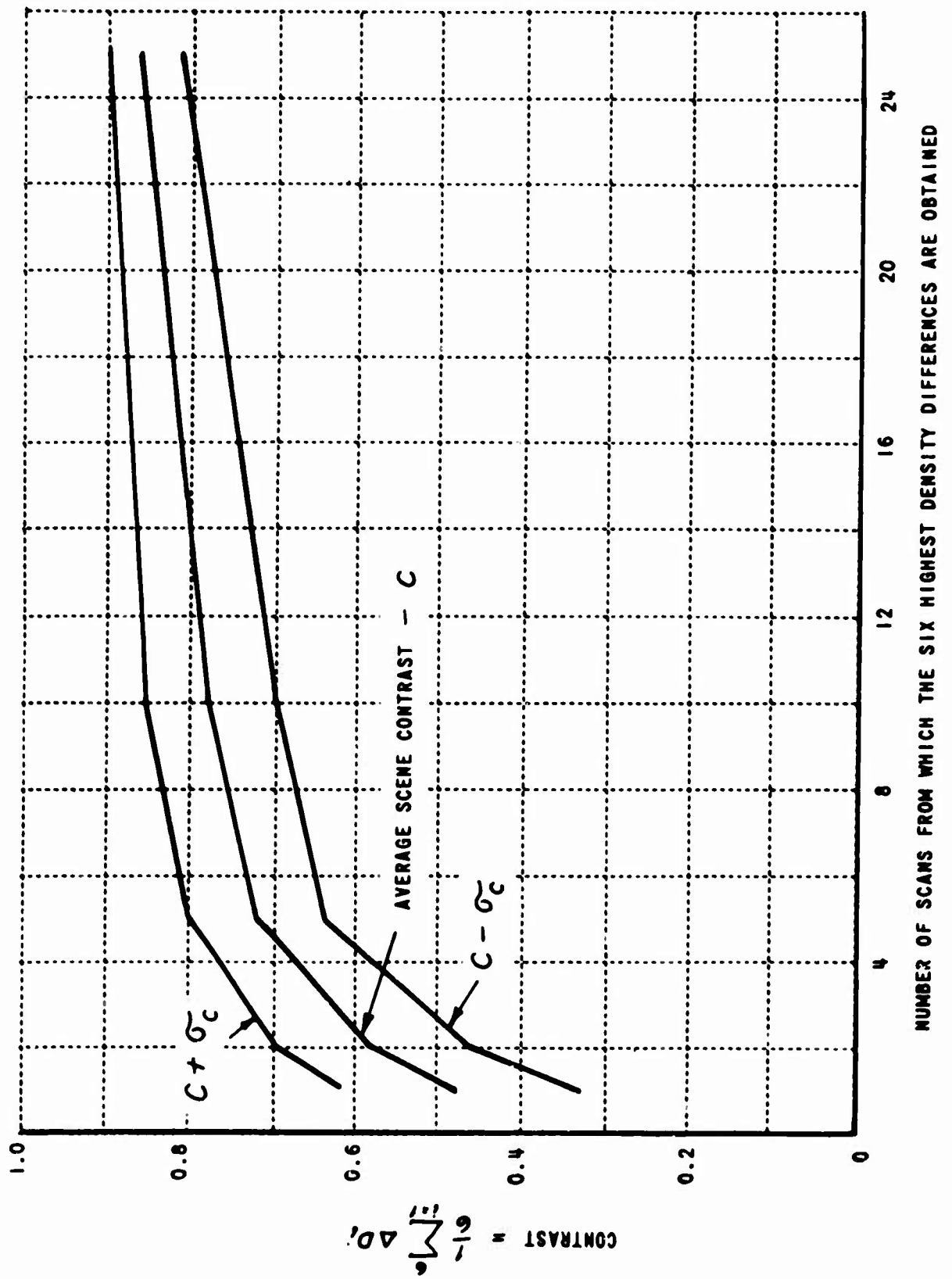


Figure 13. Contrast as a Function of Number of Scans

The measurement of this scene contrast value is accomplished in the following manner:

1. Five non-coincident scans not possessing a common intersection are made across the entire format through representative portions of the photograph using a circular aperture with an effective diameter of the order of  $2/R$  (where  $R$  is the resolution as defined earlier). The use of an aperture of this diameter results in a value of contrast which when used with the transfer function determined as in Section II A 1 above tends to compensate the errors involved in terminating an edge trace. This occurs since for a given resolution low values of  $N_e/k$  are obtained for systems which more sharply attenuate low spatial frequencies than do systems with high  $N_e/R$  values. These low spatial frequencies account for density changes over areas in the image large enough that the eye does not detect the gradient in density which exists far beyond the region of maximum density change across an edge. The eye interprets the region of low density gradient as constant density regions thus receiving the impression of lower contrast. This is illustrated in Figure 14 where two hypothetical density traces across an edge are shown. One is that expected from a system for which a high value of  $N_e/R$  would be obtained and the other for a system for which a low value of  $N_e/R$  would be obtained.

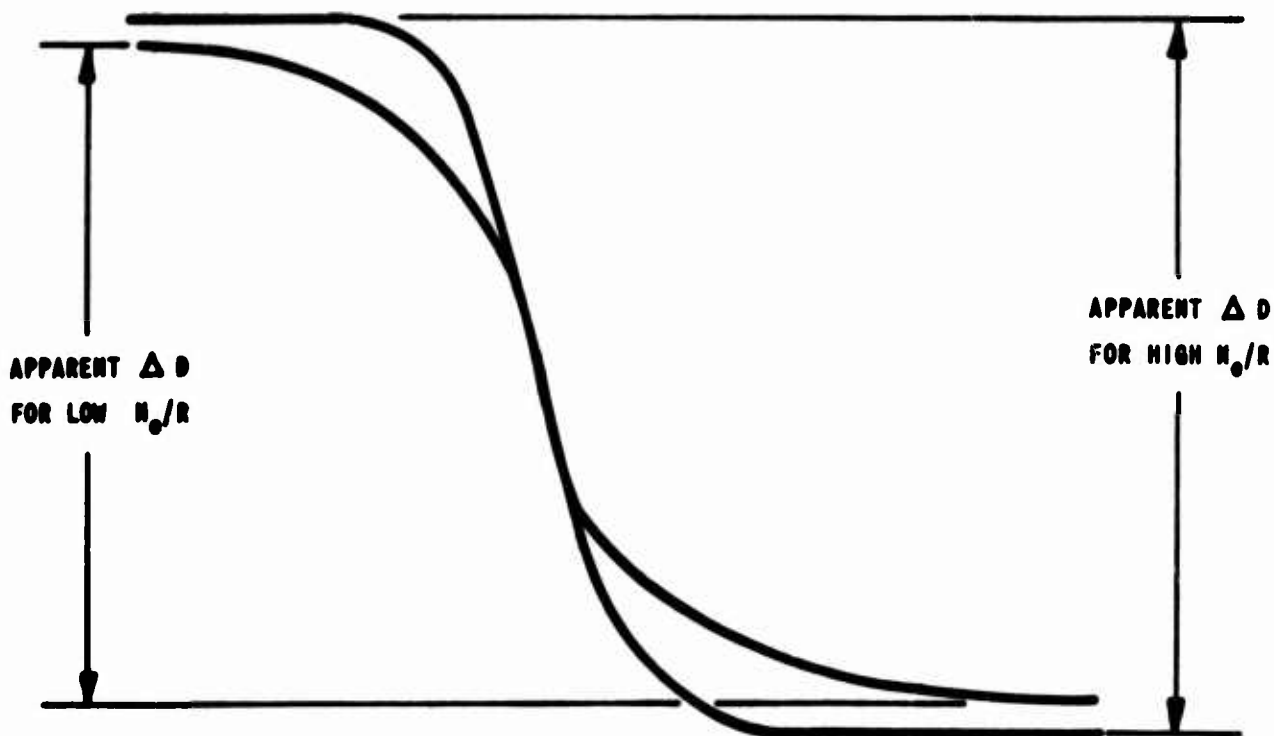


Figure 14. Apparent Density Differences For High and Low Passband To Resolution Ratios

By using an aperture of diameter  $2/R$  for the measurement of scene contrast, spatial frequencies below about  $R/2$  contribute significantly to the density fluctuations obtained from the scan of a photograph.

2. The six largest monotonic density differences in each trace are measured as indicated in Figure 15. The six largest density differences from the set of 30 obtained in the above manner are determined and their average computed.

An alternative value of scene contrast is one that is descriptive of only the contrast rendition of the system and is independent of the brightness fluctuations due to specific objects in the scene. This value of scene contrast could be multiplied by the inherent contrast of specific targets and their backgrounds to provide a value of contrast in any scene for a very specific task. The determination of the alternative definition of scene contrast has been investigated only to a limited extent. The measurement is based on the fact that large uniform areas occurring in a photograph are due to a variety of natural and man-made objects, such as for meadows, plowed fields, bodies of water and large concrete or asphalt areas. Since the reflectances of areas such as these are known the inherent contrast between any two of them can be computed. If a variety of most of the types of terrain, vegetation, and man-made objects which result in large uniformly exposed areas in an aerial photograph are considered and the average inherent contrast between all possible pairs of areas are computed, a constant value of average inherent contrast is derived. A number of aerial photographs of both rural and urban areas were examined and the

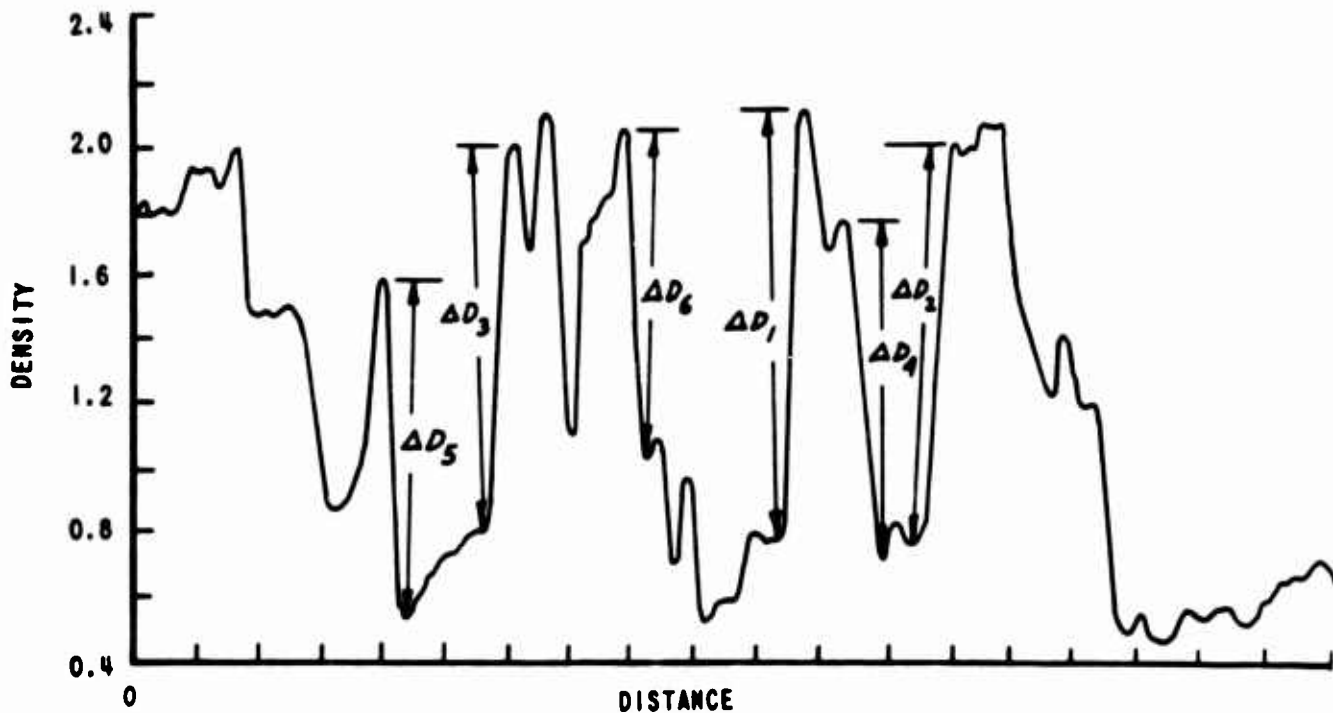


Figure 15. Typical Contrast Trace

reflectances of large areas in the scenes were postulated from a knowledge (determined by photointerpretation) of the type of terrain or vegetation causing the uniform exposure. These reflectance values were then used to compute the average contrast modulation by considering all possible pairings of areas without regard to adjacency. In all of the limited number of cases for which the average contrast modulation was computed (using as few as 5 sample areas) the value obtained was within 10% of that calculated using all available reflectance data for a large variety of terrains. This suggests that a determination of the density of several of the larger uniform areas in a photograph is all that is required to obtain data from which the scene contrast rendition can be calculated. To test this scheme, several large uniform unidentified areas were scanned on 3 photographs for which the contrast reduction factor (i. e. , the apparent contrast to inherent contrast ratio) was known. The relative exposure for each of the areas was determined from the H and D curves for the film and the average contrast modulation was computed. The ratio of this average contrast modulation to the "constant" value described above was within 10% of the known ratio of apparent to inherent contrast of the photographs.

Further testing of this technique for determining the scene contrast must be conducted to determine its limitations and reliability.

### III. SUMMARY MEASURES

The image quality parameters described in the previous section of this report each represent one facet of the total quality of a photographic image. This section describes the relationships found between measures of judged target interpretability and functional combinations (summary measures) of the quality parameters.

A visual estimation technique for determining an approximate summary measure of image quality is also discussed.

#### A. RE-EVALUATION OF Q-CAR TEST PHOTOGRAPHS

During the previous image evaluation study conducted at CAL, 1000 modified aerial photographs were produced.<sup>1</sup> These 1000 photographs consisted of twenty-five versions of each of forty different aerial scenes, with each version having different image quality parameter values. Ten representative targets were selected in each of the forty scenes and the modified photographs were then used in photointerpretation tests. In current program, eleven of the scenes (275 photographs) were selected at random and evaluated by the CAL photointerpreters who initially selected the 10 targets in each scene. No actual validation of those judgements based on ground truth was attempted. However, only those targets whose identification was independently agreed upon by three photoanalysts were used in the experiments. Their evaluation procedure was to examine each of the ten targets in each photograph and make one of the following judgments:

1. if there was no doubt that the test question could be answered;
2. if there was a high probability that the question could be answered;
3. if there was a low probability that the question could be answered;
4. if there was no doubt that the question could not be answered.

The photographs were scored by assigning to each of the 10 targets in the scene a value of 3, 2, 1, or 0, corresponding to evaluations 1, 2, 3, and 4 mentioned above. The values from the 10 targets in each photograph were summed and a percentage score was determined for each of the photographs. This percentage score (% score) is the score referred to in the remainder of this section.\*

---

\*The scores are tabulated in Appendix I.

## B. CORRELATION OF INTERPRETABILITY SCORES AND IMAGE QUALITY PARAMETERS

The % scores obtained for the 275 photographs were correlated with several functions of the image quality parameters which were considered as possible approximate summary measures of image quality. The following summary measure functions:

$$S_1 = \frac{CR}{\sigma}$$

$$S_2 = \frac{CNe}{\sigma}$$

and\*

$$S_3 = \frac{C_{\tau}(R_S)}{k\sigma\sqrt{A}}$$

(A = area of scanning aperture used to determine  $\sigma$  and  $R_S$  is the Selwyn resolution and  $\tau (R_S)$  is the value of the system transfer function at a spatial frequency of  $R_S$ .)

All generally involve the signal-to-noise ratio  $k$ , since (as mentioned in the introduction to Section II) contrast, resolution and passband are related to the signal and the granularity represents the noise. The first two measures,  $S_1$  and  $S_2$ , are the simplest to evaluate once the quality parameters have been determined. In this report the image quality parameter values determined for these photographs during the previous study are used.

The relationship between  $S_1$  and the % scores is illustrated in Figure 16. The probable error in  $S_1$  resulting from the  $\pm 30\%$  probable error in the values of  $C$  determined from the 6 highest monotonic density differences occurring in one scan across the scene (see Section II C) have also been indicated in Figure 16. The errors in the values of the other parameters are not known but are not expected to be of comparable size.

---

\* $S_3$  is equivalent in form to Selwyn's equation (Reference 5) for the sine wave resolution of a photographic system but with film "gamma" and sine wave test chart contrast modulation replaced by the scene contrast modulation  $C_M$  defined as  $\frac{(\text{Antilog } C) - 1}{(\text{Antilog } C) + 1}$  where  $C$  is the monotonic density difference scene contrast defined in Section II C of this report.

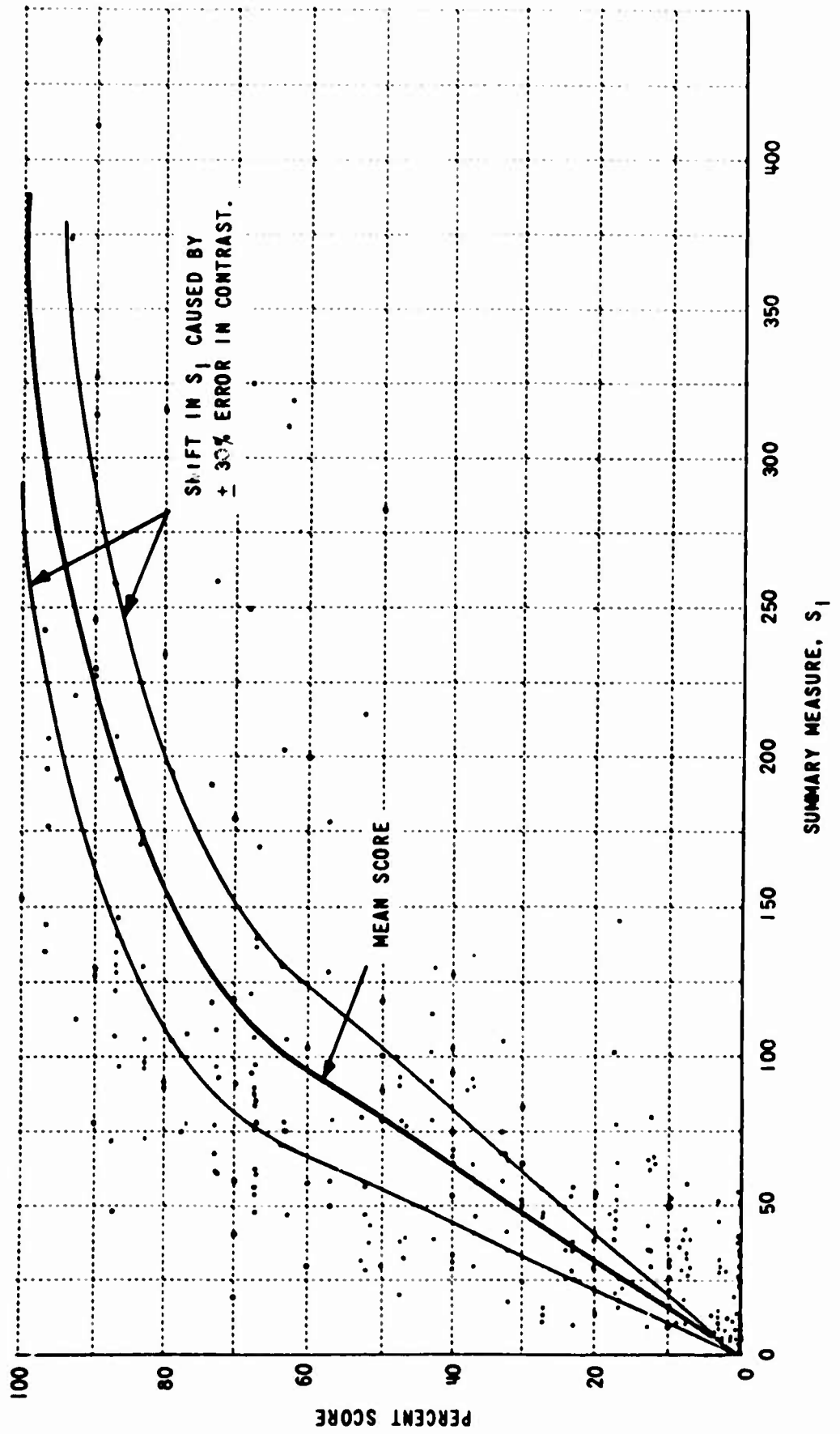


Figure 16. Correlation Of Summary Measure with Percent Score

A possible relationship (based on visual inspection of the data) between  $S_1$  and the judged interpretability scores can be inferred from Figure 16. Additional research is required to establish its reliability and to demonstrate that judged interpretability scores are predictive of direct measures of information extraction performance. Unless the latter type of correspondence can be shown, the validity of summary measures derived from the data like those of Figure 16 would remain an open question. In addition to the validation of a summary measure of image quality against one type of performance measure, it also needs to be tested against a variety of performance indices (representative of different interpretation tasks). By this means, the possible task-dependency of such a measure can be determined (i. e., different summary measures might be assigned to photography as a function of type and level of interpreter tasks).

Although inspection of a scattergram suggests some correspondence between the summary measure  $S_2$  and percent score, considerably more scatter was apparent than in the  $S_1$ -percent score relationship. While  $S_2$  incorporates all four of the image quality parameters described in Section II of this report and in Reference 1, a certain degree of redundancy exists in the use of both the values  $C$  (as determined from monotonic density differences) and  $Ne/R$ .

As explained in Section II C, the effect of  $Ne/R$ , which is descriptive of the shape of the system transfer function, is partially absorbed in the contrast measure. The effect of system passband is thus actually partially accounted for in the definition of  $S_1$ . The alternative definition of scene contrast presented in Section II C would not incorporate the effect of the passband to resolution ratio since it is a measure of the zero frequency contrast and is not affected by behavior of the transfer function at low, non-zero spatial frequencies. With regard to the effect of low spatial frequencies on the photo-interpreter, the value of  $S_2$  with this alternative definition of scene contrast thus should prove to be equivalent to the value of  $S_1$ .

The determination of the summary measure  $S_3$  involves the solution of a transcendental equation. This summary measure was computed for the photographs of only a few scenes but no apparent relationship was discernible with percent score. For these reasons no further study of this quantity was conducted.

### C. VISUAL SUMMARY MEASURE

A study was conducted to establish a technique for visually estimating the quality of photographs. In general, higher magnifications are used to examine photographs with high resolution and contrast and low granularity than for

photographs with low resolution and contrast and high granularity. The determination of the optimum magnification of a given photograph may therefore provide an approximate measure of the total image quality. The concept of "optimum" magnification for real imagery\*, however, is not easily defined and can vary with the observer. The establishment of a visual summary measure based on this concept would therefore be dependent upon a specifiable type of performance which defines "optimum" magnification for real imagery.

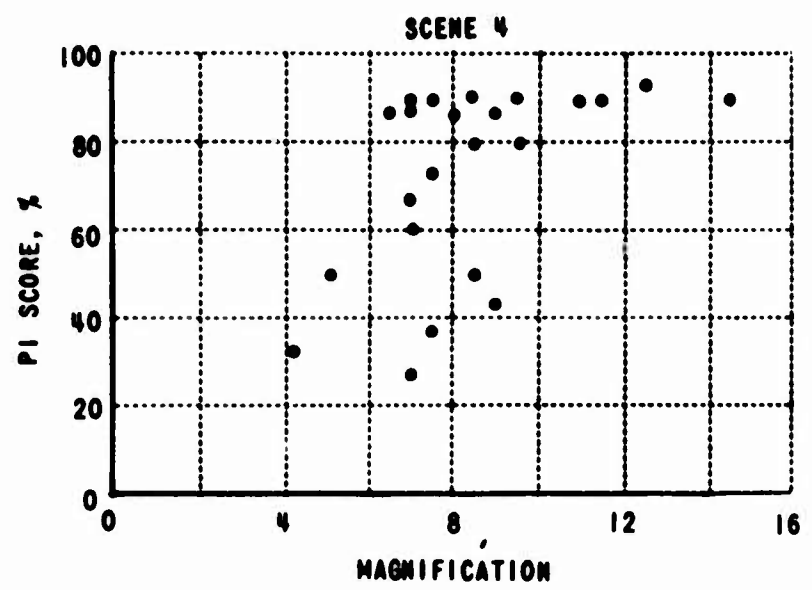
To determine such a criterion, a series of tests was performed in which a number of observers viewed 25 modified photographs of a given scene using a zoom microscope. Each was told to record the "optimum" magnification for each photograph without being told what was meant by "optimum". The criterion used by each observer was recorded and the values of magnification obtained were plotted as a function of the percent interpretability scores for each of the photographs. Three examples of the results obtained from these tests are shown in Figure 17 along with the observer's description of the criterion used to select the magnification. Although considerable variability between different observers is apparent from Figure 17, some relationship between magnification and photointerpreter performance is indicated.

Perhaps the most promising criterion which yielded the magnifications displayed in the lower scattergram of Figure 17 was viewing an edge (see Section II) in the photograph and increasing the magnification until the edge appears spread because of the resolution or discontinuous because of the grain structure of the film.

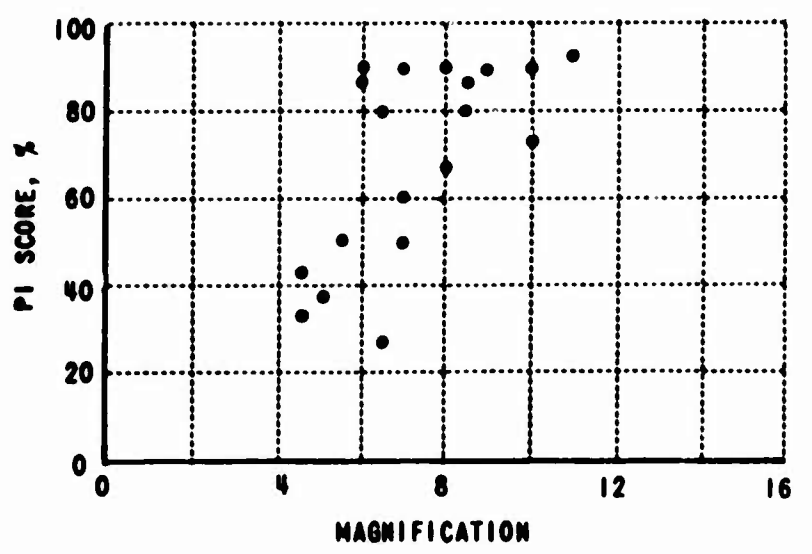
An observer not involved in the first test series was instructed to perform according to this criterion. The results obtained by this trainee, for two different scenes, are compared to the instructor's results in Figure 18. A difference in the minimum and maximum magnification used by the trainee and the instructor is shown in Figure 18. The difference in absolute magnification obtained by two persons attempting to use the same criterion, the differences in absolute magnification obtained by a single observer on subsequent trials with the same scene, and the scatter in the measurement of the magnification for any single scene indicates that the absolute magnification values do not provide a repeatable measure which could be correlated with the judged interpretability of the test photographs. The optimum magnification technique did appear to provide some rank ordering of the photographs for each scene according to judged interpretability, which was independent of the absolute level of the

---

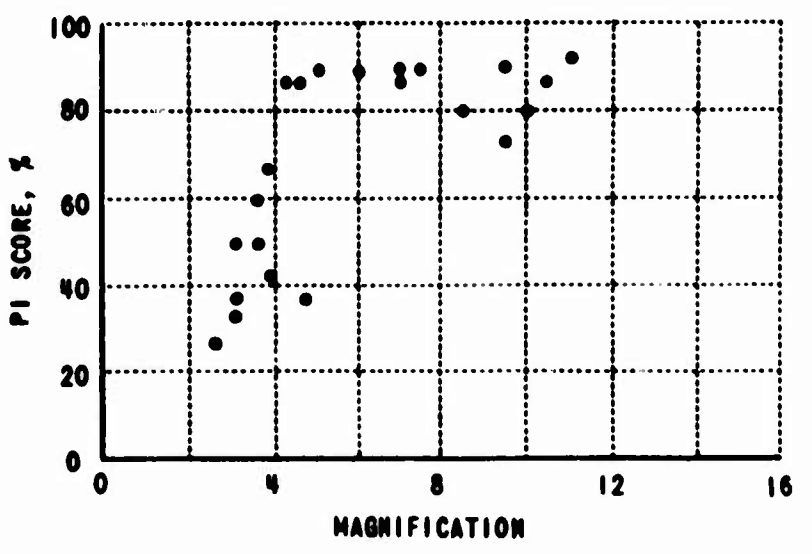
\*When viewing resolution test charts, the optimum magnification is that which enables the observer to just distinguish the last resolved set of lines or bars, i. e. when additional magnification does not enable any smaller pattern to be distinguished.



**OBSERVER 1**  
**CRITERION: MAGNIFICATION FOR APPEARANCE OF GRAIN STRUCTURE IN SMALL SCALE OBJECTS (RAILROAD BOXCARS).**



**OBSERVER 2**  
**CRITERION: MAGNIFICATION AT WHICH ROW OF SMALL OBJECTS (CARS IN PARKING LOT) COULD BE DISTINGUISHED WITHOUT EXCESSIVE DEGRADATION DUE TO GRAIN OR SYSTEM POINT SPREAD**



**OBSERVER 3**  
**CRITERION: MAGNIFICATION AT WHICH AN EDGE IN THE PHOTOGRAPH JUST BEGINS TO LOSE THE APPEARANCE OF SHARPNESS.**

**Figure 17. Optimum Magnification as A Function of Photointerpreter Performance for Different Observers and Criteria**

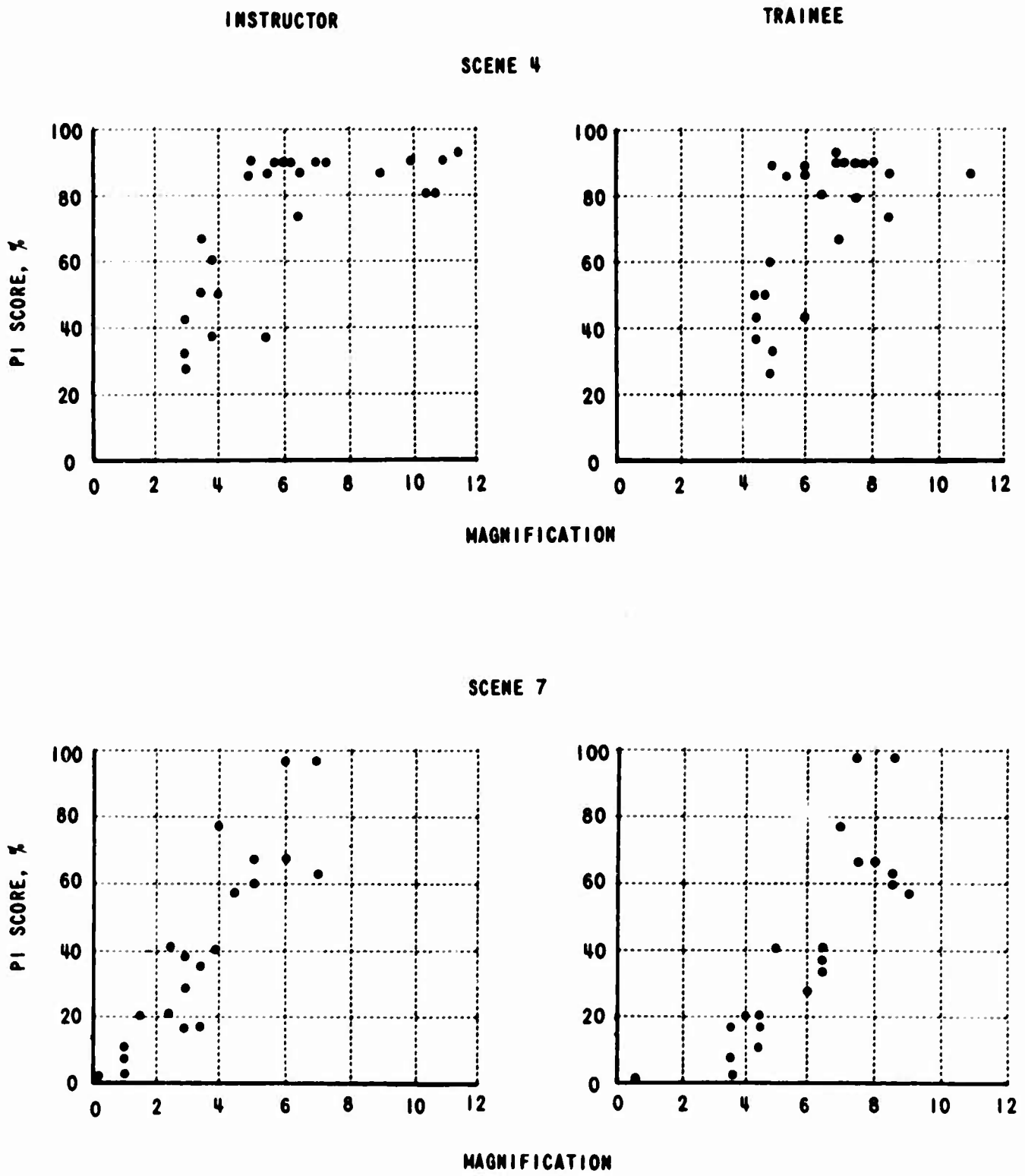


Figure 18. Comparison of Magnifications Obtained by Two Observers Using the Same Criterion

magnifications used by different observers. Rank order correlation coefficients between the ordering provided by the magnification values obtained by 3 observers for three different scenes, and the judged interpretability score ordering were computed and are presented in Table 1. A control experiment was conducted in which the sets of photographs ordered using the optimum magnification technique were again ordered without the aid of any magnification. The control experiment indicated that an observer (not necessarily a photoanalyst) can order a set of photographs without the aid of any magnification by merely comparing one photograph to another and deciding which appears to be a better photograph. The average rank order correlations with judged interpretability obtained by two observers using the unaided visual ordering technique are presented in Table 1 for three of the sets of photographs.

The data in Table 1 show that a set of photographs can be ordered according to judged interpretability by an observer using the unaided eye. The unaided visual ordering can be seen to be as good as, and in one case, significantly better than that obtained using the optimum magnification technique for the sets of photographs used.

Photographs with much higher resolutions than those of the test photographs used in this study can probably not be ordered as well by the unaided eye as they could be by using the optimum magnification criteria since the unaided eye does not resolve detail much above 10 lines per millimeter. Even in this case, however, the photographs could be compared by viewing each with a fixed magnification.

TABLE 1  
RANK ORDER CORRELATIONS

	Optimum Magnification	Unaided Eye
Scene 4	.70	.86
7	.89	.82
18	.14	.83

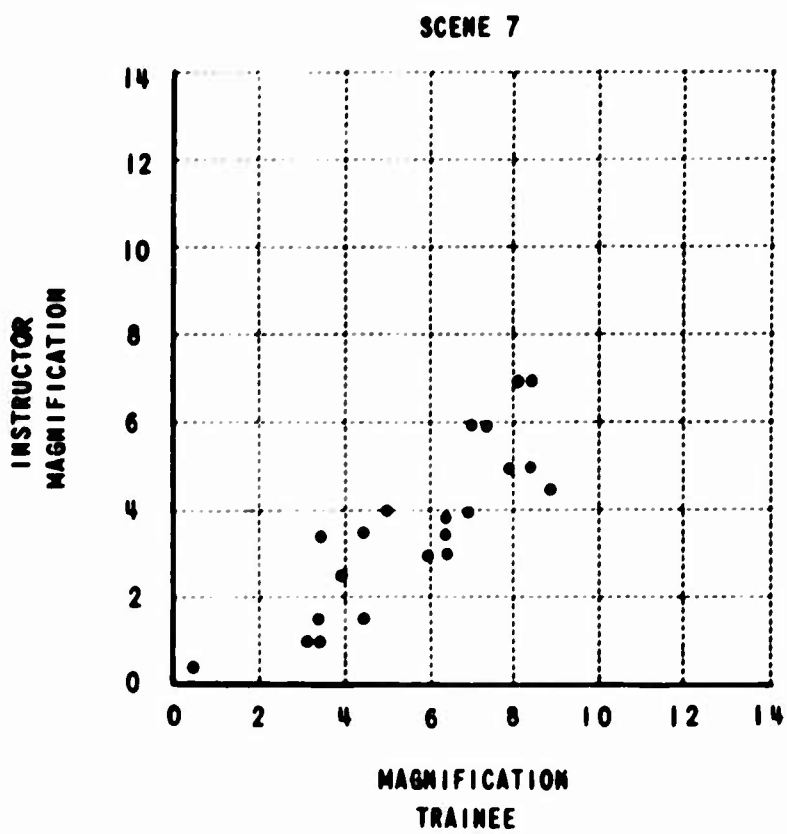


Figure 19. Correlation of Magnifications Obtained By Two Observers Using the Same Criterion

#### IV. CONCLUSIONS AND RECOMMENDATIONS

As a result of the present effort, it is concluded that:

1. Although a suggested relationship exists between quality parameters and measures of judged interpretability of aerial photographs, both the reliability and validity of this kind of relationship need to be further established.
2. The results of the visual summary measure experiments indicate that a rapid technique for ordering photographs in a set according to their judged interpretability, consists of visually comparing each photograph to the others in the set. For the cases tested, the "optimum magnification" technique, which requires more time than does the unaided eye technique, did not provide an absolute rating corresponding to judged interpretability and provided a rank ordering which is no better than the unaided eye technique.
3. A rapid, though less accurate, visual estimation technique for approximating image quality for in-field use by unskilled personnel has been developed. The method is limited to providing a gross ordering of a set of photographs according to image quality.

It is recommended that future efforts in the field of image quality assessment be oriented toward:

1. Further refinement of the data processing techniques used in the determination of the image quality parameters. Specifically in the area of optimizing numerical smoothing techniques used with edge density traces to reduce the effect of noise, and in the establishment and testing of more rigorous definitions of scene contrast.
2. Establishing the image quality necessary for satisfactory photointerpreter performance of a variety of tasks, such as a search task and identification tasks involving specific target classes.
3. Study of special problems, such as asymmetric degradations (i. e. , image motion) and color imagery.

## APPENDIX I

The values of the percentage scores for 275 test photographs re-evaluated as described in Section III are presented below. The nomenclature of the photographs is identical to that in Reference 1. The score shown for each photograph is the value agreed upon by the two photointerpreters who conducted the re-evaluation.

SCENE 4		SCENE 5		SCENE 7		SCENE 12	
P. I. *	%	P. I.	%	P. I.	%	P. I.	%
19	93	24	100	19	97	25	87
5	90	17	97	25	97	18	83
9	90	23	97	11	90	22	73
11	90	8	87	10	87	17	70
15	90	9	83	23	77	5	67
18	90	25	83	3	67	7	60
21	90	22	80	6	67	9	57
22	90	3	67	12	67	11	57
25	90	4	67	18	63	20	53
4	88	6	67	2	60	4	47
6	88	19	67	5	57	6	47
16	88	5	53	7	40	10	43
24	88	20	47	13	40	8	40
2	80	13	43	20	40	12	40
17	80	1	40	4	37	16	40
7	73	10	40	14	33	13	37
8	67	11	33	9	27	1	33
10	60	14	33	17	20	14	27
12	50	21	30	22	20	2	23
14	50	2	27	1	17	23	23
23	43	15	27	15	17	15	10
1	37	7	23	21	10	24	10
20	37	18	23	16	7	3	7
3	33	16	17	24	3	19	7
13	27	12	13	8	0	21	0

\* These numbers refer to the photointerpreter assignments in Reference 1. They are used here to retain the same identification number for each photograph.

SCENE 18		SCENE 23		SCENE 29		SCENE 30	
P. I.	%						
6	97	25	93	18	93	22	97
24	87	5	90	7	73	13	83
23	87	22	87	4	70	7	77
18	83	24	87	14	50	12	73
20	83	3	83	1	47	17	57
17	80	16	77	3	47	16	47
5	73	8	73	24	47	19	47
9	73	9	70	23	40	6	20
16	70	4	67	11	37	24	20
8	67	10	67	5	23	15	17
11	67	20	67	20	23	25	17
19	67	15	63	2	17	1	13
13	67	6	63	10	17	9	13
21	60	12	63	13	17	18	13
4	53	18	63	16	17	4	10
14	53	1	53	15	13	10	10
3	43	14	50	22	13	8	7
2	33	11	47	21	10	23	7
22	30	23	40	19	7	2	3
25	30	7	30	9	3	14	3
1	23	13	23	12	3	3	0
15	20	2	3	6	0	5	0
7	17	17	3	8	0	11	0
12	10	19	0	17	0	20	0
10	3	21	0	25	0	21	0

SCENE 31		SCENE 32		SCENE 39	
P. I.	%	P. I.	%	P. I.	%
25	70	2	67	15	77
9	67	6	67	3	73
21	52	19	67	19	73
23	52	7	63	13	70
24	20	12	63	8	47
14	17	21	63	22	43
19	13	18	57	9	37
2	7	5	53	24	37
17	7	14	53	25	37
18	7	8	50	14	30
22	7	23	50	20	20
4	3	3	43	2	17
5	3	9	40	21	17
7	3	16	37	16	10
8	3	1	23	18	10
10	3	17	17	4	7
15	3	10	13	5	7
16	3	13	13	23	7
20	3	22	10	1	3
1	0	11	7	12	3
3	0	4	3	17	3
6	0	15	0	6	0
11	0	20	0	7	0
12	0	24	0	10	0
13	0	25	0	11	0

**APPENDIX II**  
**DETERMINATION OF LINE SPREAD AND TRANSFER FUNCTIONS**  
**FROM AERIAL PHOTOGRAPHS – COMPUTER IMPLEMENTATION**

This appendix describes the calculation of the line spread and transfer functions of an optical system (including the film) utilizing the density trace of an edge occurring in the film format.

At CAL a program for an IBM 704 computer has been completed and is capable of calculating the line spread function, passband, and transfer function from edge trace data. The program is constructed with the calculations of the line spread and transfer function as subroutines in order that they may be used separately, if desired. The equations could readily be programmed for any other computer.

**PROGRAM SUMMARY**

The input consists of a data set which is a sampling of the curve:

$$D = D(x)$$

where:

D is "density"

D(x) is the "edge trace function"

Six operations are required:

1. Input of edge trace function and auxiliary data
2. Smoothing of D(x) to eliminate fluctuations due to film grain
3. Computation of the line spread function
4. Computation of the transfer function
5. Computation of the passband
6. Outputs: the edge trace function both before and after smoothing, the line spread function, passband, transfer function, and auxiliary data.

The following is a description of each of the six operations.

### Inputs

The primary input is the data set which is the sampling of the edge trace function (Figure 20). The samples are equally spaced in  $x$  and the values of  $D(x)$  lie within the interval  $0 < D(x) < 4$ . Each of the values of  $D(x)$  is expressed to the nearest thousandth (for example,  $D(x_k) = 2.563$ ). The number of samples ( $N$ ) is the order of 50, where the value of  $N$  can be different for each edge trace function.

In addition to the sampling of  $D(x)$ , auxiliary data is required as input. These are:

- (a) The value of the parameter  $\gamma$  (film gamma) used in the calculation of the line spread function (Operation 3). This parameter lies within the interval  $-10 < \gamma < 10$  and is expressed to the nearest hundredth (for example  $\gamma = 2.54$ ).
- (b) The value of  $\Delta x$  (in millimeters) between successive density data points. This value will lie within the interval  $0.01 > \Delta x > 0.00001$  and should be given to three significant figures.
- (c) Parameters useful for data smoothing (Operation 2). It may be desired to specify parameters such as:
  1. Weighting parameters
  2. Initial values to start an iterative fitting
- (d) Identification is included for each case.

### Data Smoothing

The smoothing of the edge trace function is left as a subroutine in order that the entire computer program need not be rewritten when improved smoothing routines are developed. Two alternative smoothing programs have been investigated and tested.

1. least squares fitted polynomial
2. linear filtering

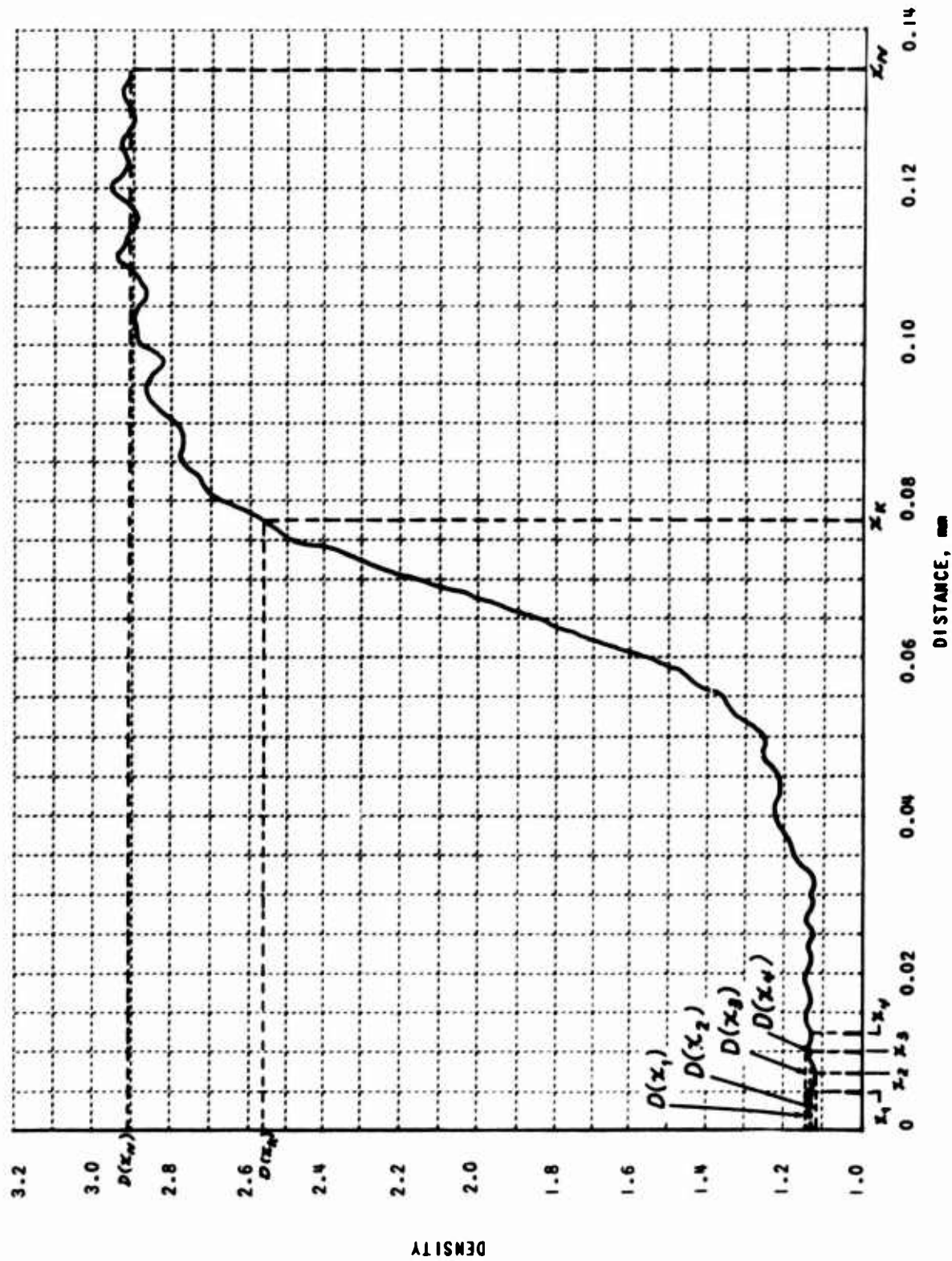


Figure 20. Sampling of Edge Density Trace

In each case the input data consist of the set of sampled densities and auxiliary parameters where needed. The output consists of the smoothed density set and the smoothed values of the derivative of the density since both of these are needed to compute the line spread function. In addition, the difference between the smoothed and unsmoothed densities at each point, and the values of certain parameters determined by the smoothing are included.

The first routine yields a set of smoothed densities of which the value at the  $k$ th sample point  $[D_s(x_k)]$  can be given by:

$$D_s(x_k) = \sum_{j=0}^M b_j x_k^j$$

where  $x_k$  is the value of  $x$  corresponding to the  $k$ th sample point. Since the sample points are equally spaced, a more convenient form for the polynomial is used,

$$D_s(x_k) = \sum_{j=0}^M a_j k^j$$

along with the derivative:

$$D_s^1(x_k) = \frac{dk}{dx_k} \sum_{j=1}^M j a_j k^{j-1}$$

The variable  $x_k$  can be written

$$x_k = (k - 1) \Delta x$$

Thus:

$$\frac{dk}{dx_k} = \frac{1}{\Delta x}$$

Therefore, the derivative  $D'_s(x_k)$  becomes:

$$D'_s(x_k) = \frac{1}{\Delta x} \sum_{j=1}^M j a_j k^{j-1}$$

The  $a$ 's are determined by minimizing the square error ( $\epsilon$ ) in fitting the polynomial. This error is written as the sum of three parts:

$$\epsilon = W_1 \epsilon_1 + W_2 \epsilon_2 + W_3 \epsilon_3$$

where  $W_{1,2,3}$  are weighting parameters specified by auxiliary input, and  $\epsilon_{1,2,3}$  are respectively the square errors in the density, the derivative of the density (end points excluded), and the derivative of the density at the end points. These part errors are given by:

$$\epsilon_1 = \sum_{k=1}^N \left[ D(x_k) - D_s(x_k) \right]^2$$

$$\epsilon_2 = \Delta^2 x \sum_{k=2}^{N-1} \left[ D'(x_k) - D'_s(x_k) \right]^2$$

$$\epsilon_3 = \Delta^2 x \left[ D_s'(x_1)^2 + D_s'(x_N)^2 \right]$$

where:

$$D'(x_k) \equiv \begin{cases} \frac{1}{2\Delta x} \left[ D(x_{k+1}) - D(x_{k-1}) \right] & (2 \leq k \leq N-1) \\ 0 & (k = 1, N) \end{cases}$$

The minimization of  $\epsilon$  leads to  $M+1$  equations,

$$\frac{\partial \epsilon}{\partial a_j} = 0 \quad (j = 0, 1, \dots, M)$$

from which the  $M + 1$  parameters ( $a_j$ ) are determined. The values selected for the parameters  $M$ ,  $W_1$ ,  $W_2$  and  $W_3$  are respectively 7, 1.0, 0.2, and 5.0.

The alternative routine (linear filtering) is accomplished by convolving the noisy density function with a function having a low pass characteristic. Since the smoothing is done after the density trace has been sampled, the convolution is written as a weighted summation over the data set:

$$D_s(x_k) = \sum_{j=-\infty}^{\infty} W(\xi_j) D(x_k - \xi_j)$$

Since the sample points are equally spaced,  $x_k$  is given as above, and  $\xi_j$  is written:

$$\xi_j = j \Delta x$$

Therefore, the smoothed density becomes:

$$D_s(x_k) = \sum_{j=-\infty}^{\infty} W(\xi_j) D(x_{k-j})$$

The weighting function was selected to have a low pass characteristic, an adjustable cut-off frequency for flexibility, and a mathematical form convenient for computer programming. The function selected is:

$$W(\xi_j) = \begin{cases} \frac{n - |j| + 1}{\sum_{j=-n}^n (n - |j| + 1)} & (-n \leq j \leq n) \\ 0 & (\text{otherwise}) \end{cases}$$

where an increase in the integer  $n$  will lower the cut-off frequency. The smoothed density now takes the form:

$$D_s(x_k) = \frac{\sum_{j=-n}^n (n - |j| + 1) D(x_{k-j})}{\sum_{j=-n}^n (n - |j| + 1)}$$

with the derivative given by:

$$D'_s(x_k) \equiv \begin{cases} \frac{1}{2\Delta x} [D_s(x_{k+1}) - D_s(x_{k-1})] & (2 \leq k \leq N-1) \\ 0 & (k = 1, N) \end{cases}$$

The above expression for  $D_s(x_k)$  requires  $D(x_k)$  be known when  $k < 1$ . These density values correspond to points lying outside the sample interval and are determined by artificially assigning them one value which is the average of the first  $2n + 1$  points within the sample region:

$$D(x_k) \equiv \frac{1}{2n+1} \sum_{j=1}^{2n+1} D(x_j) \quad (k < 1)$$

Similarly, at the other end of the sample region  $D(x_k)$  must be known for  $k > N$ :

$$D(x_k) \equiv \frac{1}{2n+1} \sum_{j=N-2n}^N D(x_j) \quad (k > N)$$

#### Computation of Line Spread Function

The line spread function,  $L(x)$ , is given in terms of the continuous density function by:

$$L(x) = \frac{D'(x) 10^{D(x)/\gamma}}{\gamma (\text{Log}_{10} e) (10^{D^+/\gamma} - 10^{D^-/\gamma})}$$

where:

$$D'(x) = \frac{dD(x)}{dx}$$

$D_+$  = density limit ( $x \rightarrow \infty$ )

$D_-$  = density limit ( $x \rightarrow -\infty$ )

In terms of the smoothed set of density values the line spread function is written:

$$L(x_k) = \begin{cases} \frac{D'(x_k) 10^{D(x_k)/\gamma}}{\gamma (\log 10 e) (10^{D(x_N)/\gamma} - 10^{D(x_1)/\gamma})} & (1 \leq k \leq N) \\ 0 & (\text{otherwise}) \end{cases}$$

#### Computation of Passband

The passband,  $N_e$ , is given by

$$N_e = \frac{1}{2} \int_{-\infty}^{\infty} L^2(x) dx$$

which is written as a summation:

$$N_e = \frac{\Delta x}{2} \sum_{k=1}^N [L(x_k)]^2$$

#### Computation of Transfer function

The transfer function,  $\tau_o(\omega)$ , is given by:

$$\tau_o(\omega) = + (\tau^*(\omega) \tau(\omega))^{1/2}$$

where:

$$\tau(\omega) = \int_{-\infty}^{\infty} L(x) e^{i\omega x} dx$$

These expressions can be written:

$$\tau_o(\omega_n) = + \left( a_n^2 + b_n^2 \right)^{1/2}$$

where:

$$a_n = \Delta x \sum_{k=1}^N L(x_k) \cos \left[ \frac{2\pi n}{N} (k-1) \right]$$

$$b_n = \Delta x \sum_{k=1}^N L(x_k) \sin \left[ \frac{2\pi n}{N} (k-1) \right]$$

$$\omega_n = \frac{2\pi n}{N \Delta x}$$

It is desired to use the spatial frequency  $\nu_n$  rather than the angular spatial frequency  $\omega_n$ . These are related by:

$$\omega_n = 2\pi \nu_n$$

Also, the exact expression for the line spread function given above (discussion of Operation 3) includes normalization to provide:

$$\int_{-\infty}^{\infty} L(x) dx = 1$$

which also yields:

$$\tau(0) = 1$$

Since the summation of  $L(x_k) \Delta x$  only approximates the integral, the value of  $a_0$  and therefore  $\tau_o(0)$ , may not be unity. Therefore,  $\tau_o(\omega_n)$  should be given by:

$$\tau_o(\omega_n) = \frac{+ \left( a_n^2 + b_n^2 \right)^{1/2}}{a_0}$$

which can be written:

$$\tau_0(\nu_n) = \frac{\left( \sum_{k=1}^N L(x_k) \cos \left[ \frac{2\pi n}{N} (k-1) \right] \right)^2 + \left( \sum_{k=1}^N L(x_k) \sin \left[ \frac{2\pi n}{N} (k-1) \right] \right)^2}{\sum_{k=1}^N L(x_k)} \quad 1/2$$

where:

$$\nu_n = \frac{n}{N\Delta x}$$

The values of  $\nu_n$  and  $\tau_0(\nu_n)$  are determined for  $n = 0, 1, \dots, N-1$ .

#### Outputs

The output includes the following:

- (a) Identification
- (b) The final values of fitting parameters involved in the data smoothing routine.
- (c) The value of  $\gamma$
- (d) A tabulation of  $x_k$ ,  $D(x_k)$  (raw data),  $D(x_k)$  (after smoothing),  $\Delta D(x_k)$  and  $L(x_k)$  for  $k = 1, 2, \dots, N$ .
- (e) The value of  $N_e$
- (f) A tabulation of  $\nu_n$  and  $\tau_0(\nu_n)$  for  $n = 0, 1, \dots, N-1$ .

For all parameters that have units, units are included in the output format. This involves  $N_e$  ( $\text{mm}^{-1}$ ),  $\nu_n$  (cycles/mm),  $L(x_k)$  ( $\text{mm}^{-1}$ ) and  $x_k$  (mm).

**APPENDIX III  
FEASIBILITY OF OBTAINING MEASUREMENTS OF  
PHOTOGRAPHIC IMAGE QUALITY FROM DENSITY  
TRACES OF EDGES\***

**1. INTRODUCTION AND SUMMARY**

This memorandum presents the results of a research program on the feasibility of obtaining measurements of photographic image quality from density traces of edges.

The measures of image quality sought are "resolution", which corresponds to the value of spatial frequency at which the transfer function has dropped to a specified value, and "passband", which is the area under the square of the transfer function. It is the purpose of this report to determine the errors incurred in these measures when certain approximations are made.

The determination of these two measures require the comparison of an "object function" occurring in the real scene to the corresponding "image function" in the film transparency. Since known test charts are absent from operational aerial photographs, simple functions, such as "points", "lines", or "edges" must be sought and recognized. True points and lines of finite intensity in the real scene are completely lost in the image but edges are not. Therefore, "degraded edges" in the image are used to obtain the two measures of interest.

Two approximations are considered; the first assumes the edge trace function is known for all values of  $x$  but the expressions relating this function to the quality measures are approximate, and the second assumes the edge trace function is known only for a finite range in  $x$ .

The first approximation is considered because the calculation of the transfer function from the density trace is a rather time consuming procedure when the exact mathematical relation is used. If the edge is of low contrast, however, a much simpler expression is available, which does not depend on film gamma, and the first case to be considered is the application of this expression to edges of high contrast and the resulting errors in the resolution and passband.

---

\* This appendix represents CAL's internally sponsored research.

The second approximation is necessary because, in practice, a microdensitometer trace of an edge is terminated at both ends, since edges in real scenes cannot be traced at large distances from the position of the step without interference from other objects in the scene format. The terminated trace, therefore, only approximates the true density function. The errors resulting in the resolution and passband, due to this approximation, are considered.

The first approximation results in simpler mathematical relations linking the resolution and passband to the density trace of an edge. The resulting value for resolution is always lower than the true value with the error ranging from 0% at low contrast to 20% at high contrast. The error introduced into the passband is shown to depend explicitly on the form of the transfer function, although upper and lower bounds have been determined. In addition, the passband errors were determined for an exponential transfer function, a gaussian, and for the transfer function corresponding to a square pulse line spread function. For all cases, the error in the passband is considerably less than the bounds indicate.

The resultant errors in the resolution and passband using the low contrast expression and the error in the resolution using the exact expression have been determined for various terminated edge traces. Closed form density functions were derived from a transfer function consisting of a linear superposition of an exponential and a gaussian and the density functions terminated by visual inspection. For all cases the approximate values were greater than the true values, with the error being negligible for a high ratio of passband to resolution, and ranging up to 20% for the resolution and 40% for the passband for a low ratio.

## 2. LOW CONTRAST APPROXIMATION

When the exposure range is assumed to lie on the linear portion of the D-log E curve, the line spread function,  $L(x)$ , can be expressed exactly in terms of a density trace,  $D(x)$ , of an edge by:

$$L(x) = \frac{D'(x) e^{\frac{D(x) - D_0}{\gamma}}}{\gamma \begin{pmatrix} \Delta D \\ e^{\gamma} - 1 \end{pmatrix}} \quad (1)$$

Where:  $\Delta D = D_1 - D_0$

$D_1$  = density limit ( $x \rightarrow \infty$ )

$D_0$  = density limit ( $x \rightarrow -\infty$ )

$\gamma = \gamma_0 (\log_{10} e)$  [ $\gamma_0$  = film "gamma"]

$$D'(x) = \frac{dD(x)}{dx}$$

If the edge is of low contrast ( $\frac{\Delta D}{\gamma} \approx 0$ ), the exponentials of Eq. (1) can be expanded, and the higher order terms dropped allowing  $L(x)$  to be written:

$$L(x) \approx \frac{D'(x)}{\Delta D} \equiv L_A(x) \quad (2)$$

The approximation results in a simple expression for  $L(x)$  which is independent of the film gamma, and therefore, it is of interest to know the accuracy with which certain image quality measures are determined due to using  $L_A(x)$  in place of  $L(x)$ , for all practical values of  $\frac{\Delta D}{\gamma}$ . The quality measures to be considered here are "resolution" (R) and "passband" (N) defined by\*:

$$R \equiv \frac{1}{2\pi} \int_{-\infty}^{\infty} \gamma(\omega) d\omega = L(0) \quad (3)$$

$$N \equiv \frac{1}{2\pi} \int_{-\infty}^{\infty} |\gamma(\omega)|^2 d\omega = \int_{-\infty}^{\infty} L^2(x) dx \quad (4)$$

\*

These quantities are similar to the "Strehl Intensity" (which correlates roughly with most measures of resolution) and Schade's "equivalent passband", respectively. Although "resolution" can be defined in other ways, the form of Eq. (3) is used for mathematical convenience.

where the position of the edge in the undegraded scene corresponds to  $x = 0$ , and  $\gamma(\omega)$  (system transfer function) and  $L(x)$  are a Fourier transform pair:

$$L(x) = \frac{1}{2\pi} \int_{-\infty}^{\infty} \gamma(\omega) e^{i\omega x} d\omega \quad (5)$$

The accuracy of these measures will be expressed, in each case, as the ratio ( $F$ ) of the approximate to the exact value:

$$F_R = \frac{L_A(0)}{L(0)} \quad (6)$$

$$F_N = \frac{\int_{-\infty}^{\infty} L_A^2(x) dx}{\int_{-\infty}^{\infty} L^2(x) dx} \quad (7)$$

a. Determination of  $F_R$

Using Eqs. (1) and (2), Eq. (6) becomes:

$$F_R = \left( \frac{e^z - 1}{z} \right) e^{-\left[ \frac{D(0) - D_0}{\delta} \right]} \quad (8)$$

Where:  $z \equiv \frac{\Delta D}{\delta}$

In general, since the exact position of the edge is unknown,  $D(0)$  and therefore  $F_R$  cannot be evaluated. However, if  $L(x)$  is restricted to be symmetric\* [ $L(x) = L(-x)$ ],  $D(0)$  can be found. Since  $L(x)$  is normalized,

\* This restriction is reasonable, since line spread functions for practical systems are usually approximately symmetric.

$$\int_{-\infty}^{\infty} L(x) dx = 1 \quad (9)$$

and symmetric  $L(x)$  allows Eq. (9) to be written:

$$\int_0^{\infty} L(x) dx = 1/2 \quad (10)$$

Substituting  $L(x)$  from Eqs. (1) in Eq. (10), and integrating:

$$e^{\frac{D(0) - D_0}{\gamma}} = 1/2(e^z + 1) \quad (11)$$

Combining Eqs. (8) and (11) yields:

$$F_R = \frac{2}{z} \left( \frac{e^z - 1}{e^z + 1} \right) = \frac{\tanh(z/2)}{z/2} \quad (12)$$

$F_R$  is plotted as a function of  $z$  in Fig. (1) and it is seen that the resolution as determined by using the low contrast approximation is less than the true resolution. The determination of the approximate resolution involves only the measurement of  $D'(0)$  and  $\Delta D$  which are obtained from a density trace that is known for all values of  $x$ . If the value of  $\gamma$  is also known the exact value of resolution can be found by correcting the approximate value with the aid of the curve in Fig. (1), or Eq. (12). If  $\gamma$  is not known exactly, but upper and lower bounds can be placed on its value (which also places bounds on  $z$ ), some correction is still possible by assuming an average value for  $z$ . Since the error in resolution varies slowly with  $z$ , widely separated bounds on this parameter will not prevent an accurate determination of the true resolution.

Even if  $\gamma$  is completely unknown, the range of values taken by  $F_R$  can be specified, since the parameter  $z$  can be related to the ratio of the exposures (known empirically for different targets) for each side of the edge in the original scene. From the Hurter-Driffield relation:

$$D = \gamma_0 \log_{10} E + k \quad (13)$$

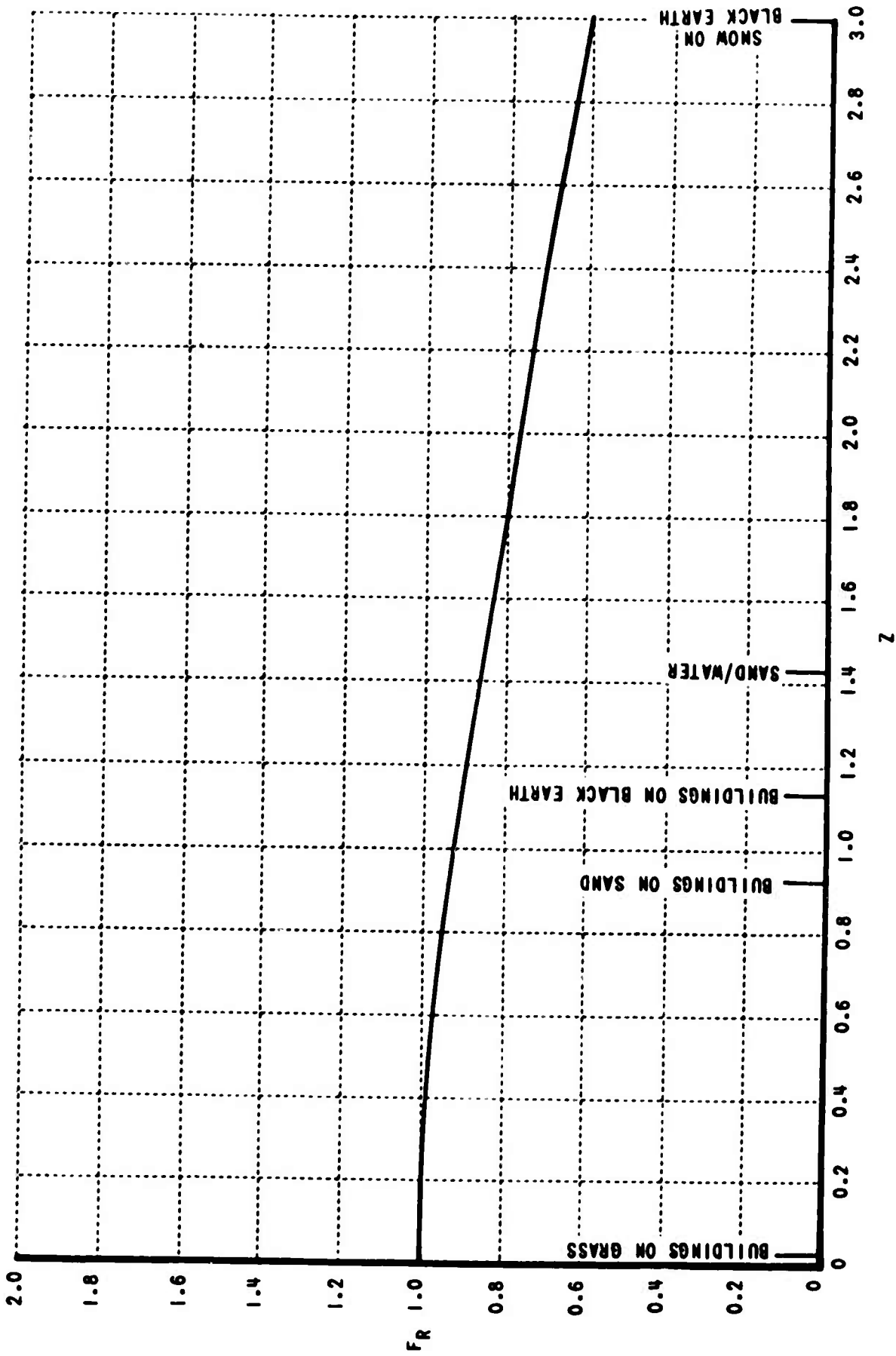


Figure 1 ERROR IN RESOLUTION

the parameter  $z$  can be expressed:

$$z = \ln \left( \frac{E_1}{E_0} \right) \quad (14)$$

where:  $E_1$  = exposure at  $x = \infty$

$E_0$  = exposure at  $x = -\infty$

Practical exposure ratios can be found by considering the spectral reflectance of various natural and man-made objects that will give rise to edges in an aerial photograph. Measurements by Krinov\* for an altitude of 1000 ft. result in specific values of  $z$ , and these are included in Fig. (1).

#### b. Determination of $F_N$

Again using Eqs. (1) and (2), Eq. (7) becomes:

$$F_N = \frac{1}{N} \left( \frac{e^z - 1}{z} \right)^2 \int_{-\infty}^{\infty} L^2(x) e^{-2 \left[ \frac{D(x) - D_0}{\delta} \right]} dx \quad (15)$$

Although the integral in Eq. (15) cannot be evaluated without knowing  $D(x)$ , upper and lower bounds can be placed on  $F_N$  by setting  $D(x) = D_0$ , and  $D(x) = D_1$ , respectively. Better upper and lower bounds can be placed on  $F_N$  when  $L(x)$  is again restricted to be symmetric. That is, since  $D(0)$  is known for symmetric  $L(x)$ , the integral of Eq. (15) can be written as the sum of two integrals; one for  $x < 0$  and the other for  $x > 0$ . An upper bound on  $F_N$  can be set by the condition:

$$D(x) = \begin{cases} D_0 & (x < 0) \\ D(0) & (x > 0) \end{cases} \quad (16)$$

and similarly a lower bound on  $F_N$  can be set by the condition:

$$D(x) = \begin{cases} D(0) & (x < 0) \\ D_1 & (x > 0) \end{cases} \quad (17)$$

\* Handbook of Geophysics, A. F. Cambridge Res. Center Chapter 14

Using these conditions (Eqs. (16) and (17) and the value of  $D(0)$  from Eq. (11)), the bounds are calculated from Eq. (15):

$$\left[ \frac{e^z - 1}{z(e^z + 1)} \right]^2 \left( \frac{5 + 2e^{-z} + e^{-2z}}{2} \right) < F_N < \left[ \frac{e^z - 1}{z(e^z + 1)} \right]^2 \left( \frac{5 + 2e^z + e^{2z}}{2} \right) \quad (18)$$

Each bound is plotted as a function of  $z$  in Fig.(2). These bounds, unfortunately, diverge rapidly for increasing  $z$ . This does not mean, however, that  $F_N$  can deviate from unity by these amounts. Better bounds should exist because it seems reasonable that the least upper bound and the greatest lower bound should have zero slope at  $z = 0$ .

Since the bounds that have been determined allow the possibility of very large errors in the passband value,  $F_N(z)$  has been computed for three specific linespread functions which are a square pulse, a Gaussian, and the line spread corresponding to an exponential transfer function. Except for the Gaussian, these functions are included in Fig. (2). The Gaussian is not plotted since the integration in Eq. (15) could not be accomplished in closed form and only two points ( $z = 0.69, 2.00$ ) were found by numerical integration. The two values, although subject to error, indicate that  $F_N(z)$  for the Gaussian is much closer to unit than either of the other two cases.

### 3. TERMINATED DENSITY TRACE

In practice, the density trace of an edge must be terminated at both ends in order to avoid interference from other nearby objects in the scene format, and it is the purpose of this section to determine the resulting errors in the measures of resolution and passband. Since the decision of where the trace should be terminated is made by visual inspection of the trace, the procedure used here to determine the errors was to calculate the resolution and passband from a visually terminated density trace and compare these results to the corresponding values for the unterminated trace. For the theoretical comparison, a convenient way of providing density traces with known resolution and passband is to derive them from a transfer function expressed in closed form. Therefore, a digression is in order to find a realistic analytic form for  $\gamma(\omega)$ .

As a starting point, the following form is considered:

$$\gamma(\omega) = \alpha e^{-|\omega|} + (1-\alpha) e^{-\omega^2} \quad (19)$$

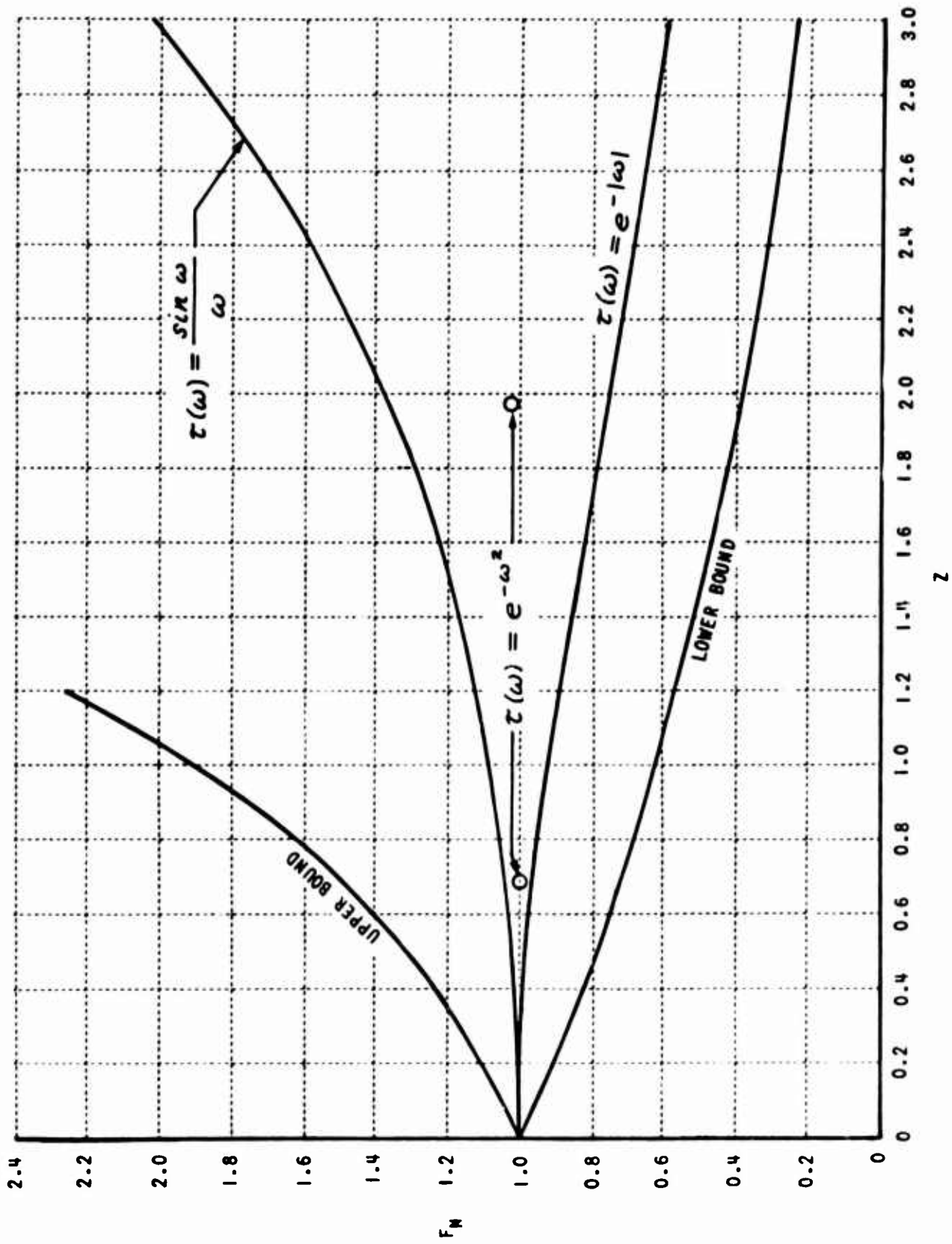


Figure 2 ERROR IN PASSBAND

This generates a family of functions in the parameter  $\alpha$ , each of which has a value of unity at  $\omega=0$  and approach zero as  $\omega \rightarrow \pm\infty$ . In addition, the form is simple, and the resolution and passband, as given by Eqs. (3) and (4), can be calculated in closed form. All that remains is to assure that this form will provide resolution and passband values consistent with those found in practice. Both the resolution and passband depend upon the scale of  $\omega$  identically, and therefore scale has been ignored in Eq. (19). What is important is the "shape" of  $\gamma(\omega)$ , and whether a significant variety of shapes is available by varying  $\alpha$ . Fig. (3) is a plot of  $\gamma(\omega)$  vs  $\omega$  for  $\alpha = 0, 1, \text{ and } 2$ , and the resulting shapes are seen to vary considerably. As discussed in the final report on Project Q-CAR, the ratio of passband to resolution is independent of scale factor and is, therefore, useful as a measure of shape. The  $\alpha$  values in the range 0-2 provide N/R values that agree with those found in practice, and, therefore the form of  $\gamma(\omega)$  given in Eq. (19) will be considered suitable for providing realistic density traces.

The errors introduced in R and N due to knowing D(x) only over a finite range of  $x$  can be related to the error in the density difference of the edge due to terminating D(x). Both the low contrast expression, Eq. (2), and the high contrast expression, Eq. (1), are considered. First, the errors in R or N will be expressed in terms of the error in the density difference for these cases. Finally, density traces corresponding to a transfer function similar to Eq. (19) are plotted from which realistic errors in  $\Delta D$ , and hence, in R and N, are determined.

The low contrast resolution as defined by Eqs. (2) and (3) can be written:

$$R = \frac{D'(0)}{\Delta D} \quad (20)$$

If D(x) is not traced for a large enough range of x, only an approximate density difference ( $\Delta_A D$ ) is known, and the error in R can be expressed by:\*

$$\frac{R_A}{R} = \frac{\Delta D}{\Delta_A D} \quad (21)$$

\* The ratios  $R_A/R$  and  $N_A/N$  used from here on should not be confused with  $F_R$  and  $F_N$  discussed earlier since the approximations are of different nature.

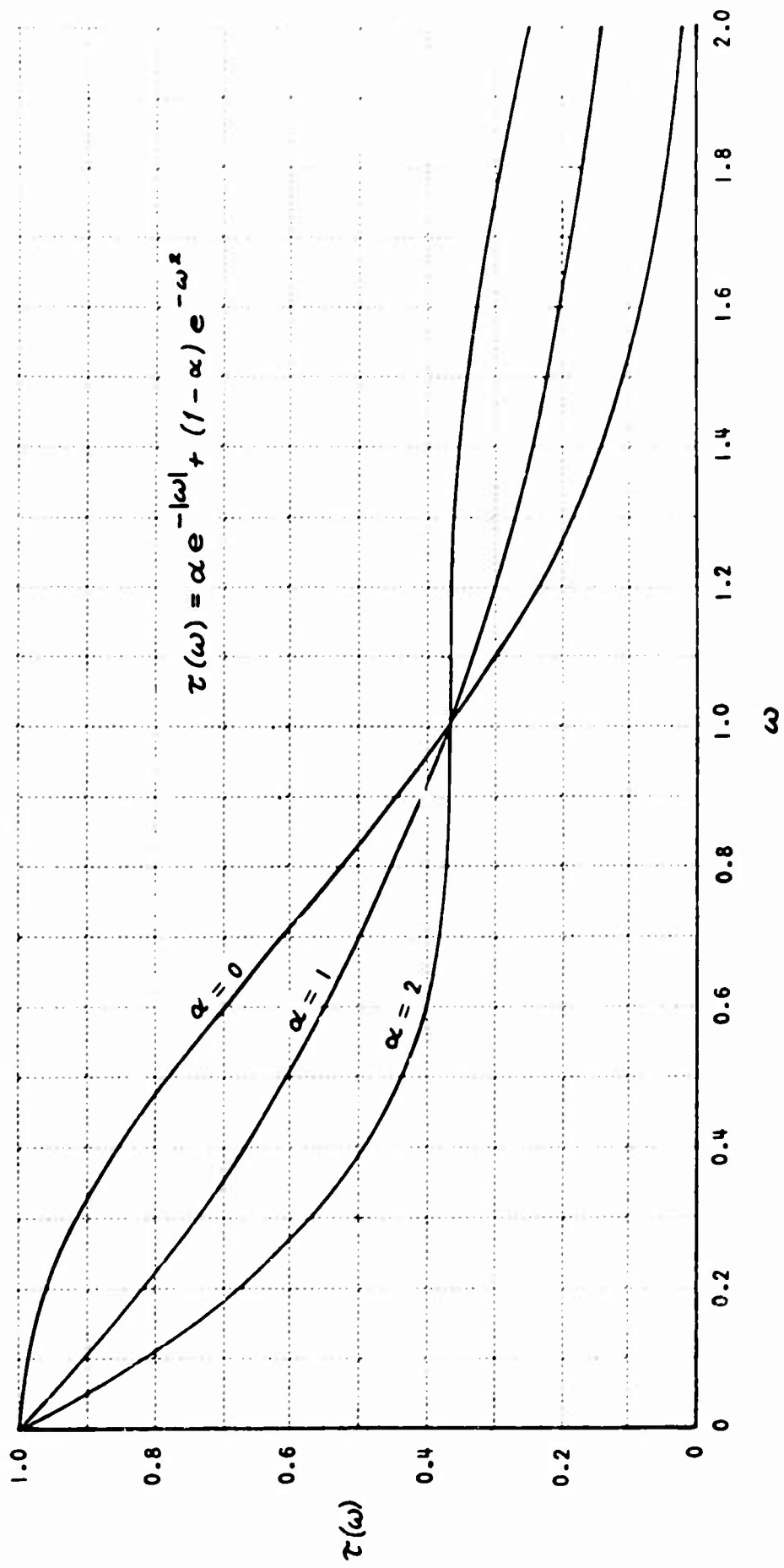


Figure 3 ANALYTIC TRANSFER FUNCTIONS

For an edge of high contrast, the exact expression for the resolution is used. From Eqs. (1) and (3) this can be written:

$$R = \frac{D'(0) e^{\frac{D(0)-D_0}{\gamma}}}{\gamma(e^z-1)} \quad \left(z = \frac{\Delta D}{\gamma}\right) \quad (22)$$

For symmetric  $L(x)$ , Eqs. (11) and (22) are combined to give:

$$R = \frac{D'(0)}{2\gamma} \left( \frac{e^z+1}{e^z-1} \right) \quad (23)$$

Again, if  $\Delta D$  is given approximately by  $\Delta_A D$  (and consequently  $z$  by  $z_A$ ) the ratio  $\frac{R_A}{R}$  can be found from Eq. (23):

$$\frac{R_A}{R} = \frac{(e^{z_A}+1)(e^z-1)}{(e^z+1)(e^{z_A}-1)} = \frac{\tanh(z/2)}{\tanh(z_A/2)} \quad (24)$$

It should be pointed out that if  $\Delta D$  is not known exactly, the position ( $x=0$ ) on the density trace corresponding to the edge in the original scene (determined by Eq. (11)) is also inexact. Although this implies an error in  $D'(0)$  of Eq. (23), this error is ignored since realistic line spread functions are slowly varying at  $x=0$ .

The calculation of the ratio of approximate passband ( $N_A$ ) to exact passband ( $N$ ) for an error in the density difference is more difficult than for the above resolutions, and only the low contrast case is considered here. From Eqs. (2) and (4) the low contrast passband can be written:

$$N = \frac{1}{\Delta^2 D} \int_{-\infty}^{\infty} D'(x)^2 dx \quad (25)$$

The approximate passband is obtained by integrating over a finite range of  $x$ :

$$N_A = \frac{1}{\Delta_A^2 D} \int_a^b D'(x)^2 dx \quad (26)$$

Where:  $\Delta_A D = D_b - D_a$

It is not possible to evaluate the integral of Eq. (26) without knowing  $D'(x)$ ; however, upper and lower bounds can be found. First, Eq. (26) can be written:

$$N_A = \frac{1}{\Delta_A^2} \left[ \int_{-\infty}^{\infty} D'^2(x) dx - \int_{-\infty}^a D'^2(x) dx - \int_b^{\infty} D'^2(x) dx \right] \quad (27)$$

An upper bound is obtained by letting:

$$\int_{-\infty}^a D'^2(x) dx = \int_b^{\infty} D'^2(x) dx = 0 \quad (28)$$

Therefore, from Eqs. (25), (27), and (28):

$$\left( \frac{N_A}{N} \right)_{MAX} = \left( \frac{\Delta D}{\Delta_A D} \right)^2 \quad (29)$$

A lower bound results from rewriting the last two integrals of Eq. (27) and making the reasonable assumption that in the ranges  $x < a$  and  $x > b$ ,  $|D'(x)|$  decreases monotonically as  $x \rightarrow \pm\infty$ . These integrals can then be written:

$$\left. \begin{aligned} \int_{-\infty}^a D'^2(x) dx &= \int_{D_0}^{D_a} D' dD < D'(a) (D_a - D_0) \\ \int_b^{\infty} D'^2(x) dx &= \int_{D_b}^{D_1} D' dD < D'(b) (D_1 - D_b) \end{aligned} \right\} \quad (30)$$

Eqs. (25), (27), and (30) yield:

$$\left(\frac{N_A}{N}\right)_{MIN} = \left(\frac{\Delta D}{\Delta_A D}\right)^2 - \frac{D'(a)(D_a - D_o) + D'(b)(D_i - D_b)}{N \Delta_A^2 D} \quad (31)$$

From Eqs. (29) and (31) it is seen that the right hand term of Eq. (31) is the difference between the two bounds. It will be shown below that for reasonable terminating points this term is small, and the bounds become identical, thereby determining  $\frac{N_A}{N}$ .

In order to obtain a feeling for the magnitude of the error in determining  $\Delta D$ , edge density traces representing low, medium, and high ratios of  $N/R$  are plotted in Figs. (4) and (5). These curves were derived from a transfer function of the form:

$$\gamma(w) = \alpha e^{-(\ln 4)|w|} + (1-\alpha) e^{-(\ln 4)w^2} \quad (32)$$

The curves are plotted for a film gamma ( $\gamma_o$ ) of 2, and density differences ( $\Delta D$ ) of 0.60 (Fig. (4)) and 1.74 (Fig. (5)). In each case the ratio  $N/R$  is varied by allowing  $\alpha$  to take values of 0, 1 and 2. For each of the six curves, estimates of the terminating points were made by visual inspection. These points were selected in the same regions as would be done for traces from real scenes where the tails of the traces might be affected by the presence of neighboring objects. These values, along with the resulting ratios  $\frac{R_A}{R}$  for both the low and high contrast cases, and  $\frac{N_A}{N}$  for the low contrast case, are included in Table (1). With regard to the last ratio ( $\frac{N_A}{N}$ ), the selected terminating points resulted in values of  $D'(a)$  and  $D'(b)$  small enough that the last term of Eq. (31) is less than 1/2% of the first term for all six cases. Therefore, the last term can be ignored, which results in identical upper and lower bounds on the parameter  $\frac{N_A}{N}$ . Thus:

$$\frac{N_A}{N} = \left(\frac{\Delta D}{\Delta_A D}\right)^2 \quad (33)$$

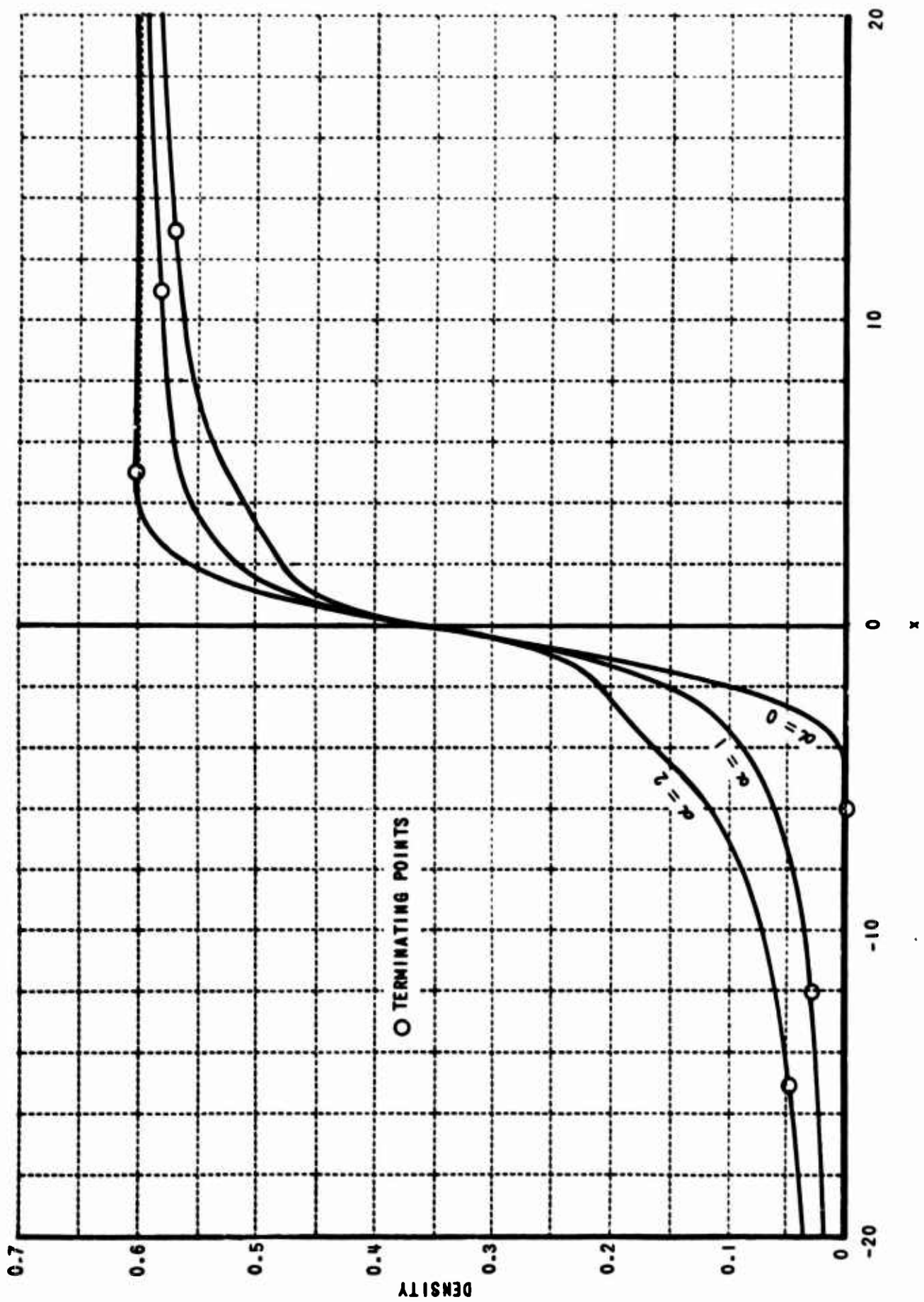


Figure 4 DERIVED DENSITY TRACES ( $\Delta D = 0.60$ )

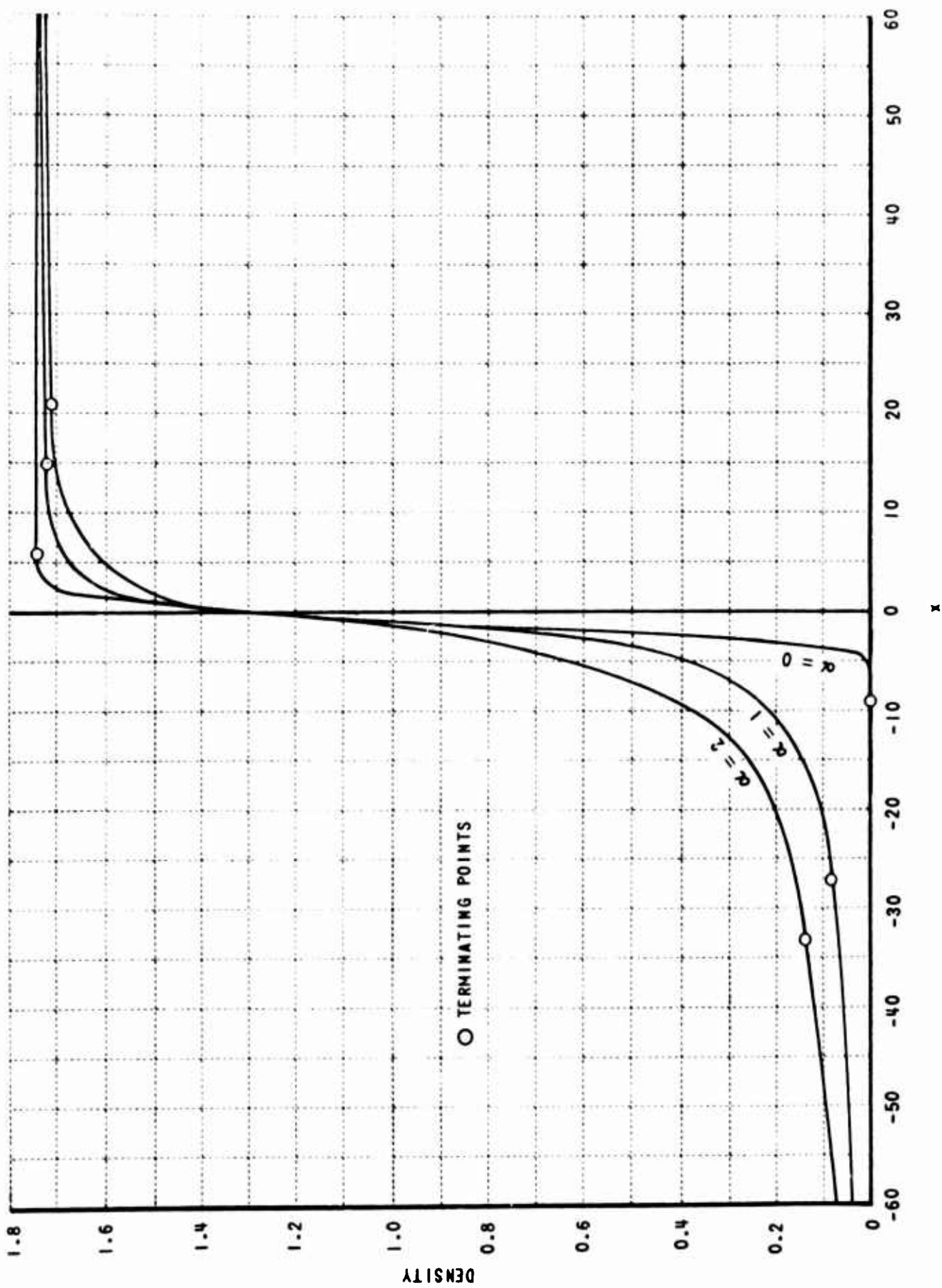


Figure 5 DERIVED DENSITY TRACES ( $\Delta D = 1.74$ )

$\Delta D$	$\alpha$	$a$	$b$	$\Delta_A D$	$\frac{R_A}{R}$ (low contrast)	$\frac{R_A}{R}$ (exact)	$\frac{M_A}{N}$
0.60	0	-6.0	5.0	~0.60	~1.00	~1.00	~1.00
0.60	1	-12.0	11.0	0.55	1.09	1.06	1.19
0.60	2	-15.0	13.0	0.51	1.18	1.16	1.39
1.74	0	-9.0	6.0	~1.74	~1.00	~1.00	~1.00
1.74	1	-27.0	15.0	1.63	1.07	1.04	1.14
1.74	2	-33.0	21.0	1.54	1.13	1.07	1.28

TABLE (1)

#### 4. RESULTS

The expression derived for low contrast edges provides a simple relation between the density trace and the line spread function which is independent of film gamma, and its use as an approximation for edges of higher contrast results in the following errors in resolution and passband:

- (1) The resultant resolution values are always less than the true values, with an error of less than 15% for most edges occurring in aerial scenes.
- (2) Errors in the resolution values can be reduced when an approximate value of film gamma is known.
- (3) For sample cases considered, the resultant passband values were in error by less than 20%, however, no general limits could be derived.

The errors introduced into the resolution and passband values by a lack of knowledge of the density trace far from the edge depend on the error in evaluating the total density difference ( $\Delta D$ ) across the edge:

- (1) The error in estimating  $\Delta D$  increases as the ratio of passband to resolution decreases.
- (2) The % error in the resultant resolution is equal to the % error in  $\Delta D$ , and can be as high as 20% for the lowest practical passband to resolution ratios.
- (3) The % error in the resultant passband is equal to twice the % error in the resolution error.

#### 5. CONCLUSION

It is concluded that, within the accuracy required by image quality measures for most applications, an edge trace is a good source of these measures. Moreover, since the errors resulting from the use of the low contrast expression are comparable to those created by the termination of edge traces, the low contrast expression can be used whenever convenient.

#### 6. RECOMMENDATIONS

(1) At present, there is no quantitative criterion for selecting termination points of a density trace. A method should be developed to perform this selection and the resulting errors in resolution and passband re-evaluated.

(2) Realistic density traces should be examined to determine if the true total density difference can be correlated with the behavior of the trace in the sampled region. If a correlation can be found, the error in the density difference, and therefore in resolution and passband, can be reduced.

## REFERENCES

1. Roetling, P.G., Hammill, H.B., and Holladay, T.M., "Quality Categorization of Aerial Reconnaissance Photography", CAL Report No. VE-1667-G-1, Final Report, Contract No. AF 30(602)-2684, 30 September 1963.
2. Parry, Peter D., "Image Modification by Spatial Filtering", Technical Documentary Report No. RADG-TDR. To be published.
3. Hammill, H.B., and Holladay, T.M., "Feasibility of Obtaining Measurements of Photographic Image Quality From Density Traces of Edges", Internal Research Study, CAL Report No. CAL-132. To be published.
4. Fleck, J.T., and Fryer, W.D., "An Exploration of Numerical Filtering Techniques", Internal Research Study, CAL Report No. XA-869-P-1, 1 May 1953.
5. Selwyn, E.W.H., "The Photographic and Visual Resolving Power of Sensors", Photographic Journal, Vol. 88B, (1948), pp. 46-57.